PROGRESS REPORT ON

IN-74-86

Application of Landsat TM images to assess circulation and dispersion in coastal lagoons.

(NAS5-28741)

Submitted to

National Aeronautics and Space Administration

NASA/Goddard Space Flight Center

Code 602

Greenbelt, MD 20771

Attention: Dr. Harold Oseroff

Björn Kjerfve, John R. Jensen, and K.E. Magill

Belle W. Baruch Institute for Marine Biology

and Coastal Research

University of South Carolina

Columbia, SC 29208

15 February 1986

(NASA-CR-177315) APPLICATION OF LANDSAT TM IMAGES TO ASSESS CIRCULATION AND DISPERSION IN COASTAL LAGOONS Progress Report (South Carolina Univ.) 38 p HC A03/MF A01 CSCL 08C

N86-26665

Unclas

G3/43 43291

SUMMARY

The University of South Carolina investigation under auspices of the NASA TM Announcement of Opportunity project is progressing well and is on schedule. Our only difficulty is associated with obtaining new TM scenes. The project is presently in its 7th month (formal starting date was 18 July 1986).

The main objectives of this 24-month study are formulated around a four-pronged work approach, consisting of tasks related to:

1) image processing and analysis of Landsat TM data;
2) numerical modeling of circulation and dispersion;
3) hydrographic and spectral radiation field sampling/ground truth data collection;
4) special efforts to focus the investigation on turbid coastal/estuarine fronts.

So far, we have made the most progress in task 2, numerical modeling of circulation and dispersion of salinity and suspended sediments in Laguna de Terminos, Mexico, and Lake Calcasieu, Louisiana, our two primary study sites. We have examined three Landsat TM scenes received from NASA, and have carried out preliminary analysis on two of these covering Laguna de Terminos, Mexico (ID# Y5026915590), and Lake Calcasieu, Louisiana (ID# Y5027416142). We have a need for 8 more scenes.

We are now preparing for the collection of ground truth data in Laguna de Terminos. A 2-week sampling period has been scheduled for 8-21 March, 1986, and we have requested and hope to obtain a Landsat TM scene for this lagoon coinciding with our field data collection.

NUMERICAL MODELING

Most of our effort thus far has been allocated towards development and implementation of the 2-D, vertically-integrated, finite difference estuarine tidal model (modified after: Blumberg, A.F. 1977. Numerical tidal model of Chesapeake Bay. J. Hydraulics Div., Proc. ASCE, HY1: 1-10) and accompanying dispersion model. The governing equations of the hydrodynamics model are the global shallow water equations (Welander, P. 1957. Wind action on a shallow sea: some generalizations of Ekman's theory. Tellus 9: 45-52.), which result after vertical integration of the momentum balance equations. The equations are unsteady, retain the non-linear field acceleration terms, and include earth rotation, barotropic pressure gradients, wind stress, non-linear bottom friction, and horizontal diffusion of momentum. Both models are driven by tides, wind stress, and river discharge, and have the capacity to simulate vertically averaged longitudinal and lateral velocity patterns, tidal elevation distributions, and concentration distributions/fluxes for passive, conservative constituents.

The model results may be output as several different graphics products. These include residual plots of water elevation, salinity, and suspended sediment contours, and vectoral velocity plots of net (tidally averaged) velocities, Stoke's (tidal wave induced) velocities, and residual transport velocities (net minus Stoke's). Each velocity representation may be plotted as either dimensional point vectors or non-dimensional streamlines. The residual plots may be computed over any specified averaging period. For both lagoons, we averaged over 1 diurnal tidal cycle (24.84 hr). However, to ensure that the computations have reached quasi-steady state, it is first necessary to run the simulation computations for at least 15 tidal cycles.

Instantaneous values of water elevation, salinity, suspended sediments, and velocity may also be plotted for any given time interval, and time series of these values may be created at any number of specified grid points and at any desired sampling rate. This time series utility will be used extensively when calibrating/verifying the model with ground truth and Landsat TM data.

Both models are presently working satisfactorily on both Laguna de Terminos and Lake Calcasieu. We have completed several model runs under simulated conditions for both lagoon systems.

Four model runs have been completed on Laguna de Terminos, simulating the mixed, mainly diurnal tidal regime and 1) trade wind conditions with mean river discharge; 2) no winds with mean discharge; 3) "norte" winds with mean discharge; and 4) no winds and flood discharge conditions. These conditions are representative of the range of situations known to occur throughout the year in this region. The attached manuscript (see Appendix I) describes the hydrodynamics/dispersion model in full detail, and presents the time-averaged results from the four simulation runs on Laguna de Terminos.

Two runs have been completed on the Lake Calcasieu system, simulating hydrodynamic/dispersion conditions which may occur during 1) a no wind case; and 2) winds from the north at 360^{0} and 10 m/s. Mean discharge values at the river mouths and diurnal tidal components were input for both cases. Examples of generated graphics outputs from the Lake Calcasieu simulation runs are provided in the Appendix II.

The numerical modeling is carried out on a VAX 11/780 under VMS. The computer is maintained by the University of South Carolina Computer Services Division. We access the machine interactively from terminals in the Physical Oceanography Laboratory.

IMAGE PROCESSING

All image processing is being carried out in the Remote Sensing Laboratory of the Department of Geography. The equipment consists of an IBM AT microcomputer with a 20 Mb hard disk, in conjunction with an ERDAS image processing system and ERDAS Digital Image Processing and GIS software from Earth Resource Data Analysis, Inc. in Atlanta, GA; a 1600 bpi tape drive; and a Modgraph Color Camera for the preparation of instant, Polaroid 35 mm, 4 x 5", 8 x 10" negative and positive transparencies of the CRT screen.

Our image analysis has only recently begun in earnest because of prior time commitments on the image processing system. So far, we have focused our attention on two scenes, one each of Laguna de Terminos (from 25 Nov 1984) and Lake Calcasieu (from 30 Nov 1984). Our initial analysis consists of image rectification, contrast stretching the data in each of bands 1 - 4, and producing density-sliced pseudo-color images of each of the single bands, as well as several different combinations of bands. We have not yet made atmospheric corrections to the data, but plan on doing so with the next requested TM image of Laguna de Terminos, which ideally will coincide with our field sampling effort. Our next step is to run the models using historical input data from the respective days of the two images, and compare our model-simulated suspended sediment contours with color gradients derived from the density-sliced images. We are not providing any samples of the image analysis with this progress report, but intend to do so in our next progess report.

TM DATA REQUIREMENTS

At present, we have received from NASA the following Landsat TM data products:

1) CCT-PT, 024/039, 30 NOV 1984 (Lake Calcasieu), quadrants 3,4
2) CCT-PT, 021/047, 25 NOV 1984 (Laguna de Terminos), quadrants 1,2,3,4
3) CCT-PT, 019/047, 11 NOV 1984 (Chetumal Bay), quadrant 3

Tapes 1 and 2 (Lake Calcasieu and Laguna de Terminos) are of high quality, with zero cloud coverage over the lagoons, and only a few bad data points. These scenes are of excellent quality for image processing and analysis. However, tape 3 contains a high percentage of cloud cover and haze, and it will be difficult to use in our analysis.

The following list of Landsat TM products have been requested, but have not been received at this time:

1) CCT-PT, 016/037, 14 May 1984 (Charleston Harbor).
   We received the wrong tape from NASA (Charleston, W.VA instead of Charleston, SC), and have returned it to be exchanged with our initially requested scene. It is our intention to use this image for testing of hypotheses relative to the turbid coastal boundary layer frontal structure.

2) CCT-PT, 021/047 (Terminos Lagoon), March 1986 acquisition.
   Per telephone call to Maria Mackie on 22 Jan 1986, we have been promised a March 1986 TM acquisition of this path/row, provided the

data are of good quality. For two weeks in the beginning of March, we will be collecting field data from the lagoon. Obtaining a scene from this time period is therefore a critical component to our collection of ground truth data for Laguna de Terminos.

3) CCT-PT, 021/047 (Terminos Lagoon), Jul-Sep 1985 acquisition.
We ordered this acquisition on 26 May 1985, and were notified by Maria Mackie of 2 scenes from September of acceptable quality. We ordered these. However we have now been informed that NASA cannot obtain these data sets for our use due to negotiations with EOSAT. This is potentially a major loss to our research. We originally anticipated and requested several more acquisitions of data from this study area. We would like to have coverage of the "norte" season in November, the March dry season, the September wet season, and one more season coinciding with our field work.

4) CCT-PT, 024/039 (Lake Calcasieu), Jul-Sep 1985 acquisition.
On 26 May 1985 we ordered an acquisition during the above time period, but have not received any data.

5) B/W negative transparencies (TM band 4) for each CCT ordered.
We ordered these as an aid in locating our study areas on the tapes, and to assess quickly the cloud coverage over the study sites. These were ordered in 1985, but again, we have been notified that NASA cannot obtain these products for us.

We have been informed via Maria Mackie that, due to the recent change of Landsat data ownership to EOSAT, each investigator will now only receive from NASA at most 2 more Landsat TM CCT's for their research. We would hope to be able to obtain 8 more scenes. In our original proposal, we anticipated a need for 12 scenes: 6 from Laguna de Terminos, and 2 each from Lake Calcasieu, Lagoa dos Patos, and Lake Songkla. In retrospect, 4 scenes from Laguna de Terminos is a reasonable compromise. Therefore, at least 3 more additional TM scenes from Laguna de Terminos are needed to have representations of the major hydrographic regimes. We would also like to have one more image of Lake Calcasieu and one full coverage each from Lagoa dos Patos and Lake Songkla (two adjacent TM scenes per area). We have not yet requested scenes from these latter two areas but hope to do so in the near future when NASA can provide us with more data products. We are waiting for the launch of the TDRSS-West to be able to specify a scene from Lake Songkla.

In summary, we would ideally like to obtain the following number of <u>additional</u> TM data products:

a) Laguna de Terminos: 3 scenes

b) Lake Calcasieu: 1 scene

c) Lagoa dos Patos: 1 coverage (area covers two adjacent TM scenes)

d) Lake Songkla: 1 coverage (area covers two adjacent TM scenes)

e) B/W negative transparencies (TM band 4) for each of above CCT's.

FIELD DATA COLLECTION

From June 1984 until January 1985, an intensive hydrographic field survey was conducted in the Lake Calcasieu system, utilizing equipment from the University of South Carolina. The purpose of the field investigation was to obtain time series measurements of velocity, tidal elevation, and density under auspices of a Department of Energy (DOE) contract. We used 4 internally recording pressure-type (SOI Mark V) tide gauges, an SOI Mark VIII current meter with CT capability and internal recording, and 2 ENDECO neutrally buoyant current meters for current and CT measurements. These instruments were moored at locations throughout the Lake Calcasieu system for the entire survey period. We had problems with the moorings because of heavy barge traffic, shrimp fishing, and recreational fishing. Several of our instruments were damaged, destroyed, or lost. However, we were able to obtain useful 29-day tidal records and current/CT records at some of the mooring sites. These data are now being analyzed to be used to calibrate/validate the numerical model performance.

We are traveling to Cd. del Carmen, Mexico from 8 - 20 March, to gather field/ground truth data from Laguna de Terminos. The purpose of this field survey is to collect the necessary measurements for calibration/verification of both the model and the Landsat TM data. We have made arrangements to stay and carry out operations at the marine field station, Estacion El Carmen/UNAM, which is equipped with boats and some instrumentation for conducting field work. As already mentioned, we hope to obtain a Landsat TM image of this study area (path/row 21/47) from 17 March 1986. We are coordinating our field work with the time of this satellite overpass. Normally, March is a dry

period and weather conditions should be optimum for the acquisition of cloud-free Landsat TM data. Field neasurements will include salinity, total suspended sediments, currents, tidal elevations, turbidity, and in situ radiometric data.

To obtain more data on the structure of turbid fronts, we intend to make several hydrographic transects through the coastal boundary layer front at Charleston, SC. The technique for conducting these measurements and the associated analyses will then be applied to the Laguna de Terminos field and TM data.

PURCHASE OF PROJECT EQUIPMENT

We have received all equipment ordered under the auspices of this grant. This includes:

1) Spectron Engineering Model SE590 Portable Spectroradiometer: including a spectral detector head with a spectral range of 400 - 1100 nm, a microprocessor based controller and portable data logger, and software options, including a Thematic Mapper band simulator;
2) InterOcean model S4 current meter: a spherical, self-contained electromagnetic current meter with solid state memory, microprocessor control, and optional temperature, conductivity, and pressure sensors; and
3) Monitek model 21PE portable nephelometer.

In addition to these newly purchased instruments, other existing equipment will be used in the field work.

PROJECT PUBLICATIONS

Two manuscripts have resulted to date from this NASA project. They are attached as appendices. The full references are:

Kjerfve, B. In press. Comparative oceanography of coastal lagoons. In: Estuarine Variability. D.A. Wolfe (ed.). Academic Press.

Kjerfve, B., K.E. Magill, and J.E. Sneed. Modeling of circulation and dispersion in Laguna de Terminos, Campeche, Mexico. In press. In: Ecology of the Southern Gulf of Mexico Coastal Zone with Special Reference to the Terminos Lagoon Region. A. Yáñez-Arancibia (ed.). Universidad Nacional Autonomas Mexico.

APPENDICES

1. Kjerfve, B., K.E. Magill, and J.E. Sneed. Modeling of circulation and dispersion in Laguna de Terminos, Campeche, Mexico. In press. In: Ecology of the Southern Gulf of Mexico Coastal Zone with Special Reference to the Terminos Lagoon Region. A. Yáñez-Arancibia (ed.). Universidad Nacional Autonomas Mexico.

2. Sample graphics simulation outputs from Lake Calcasieu model runs.

3. Kjerfve, B. In press. Comparative oceanography of coastal lagoons. In: Estuarine Variability. D.A. Wolfe (ed.). Academic Press.

APPENDIX I

(Publication on Laguna de Terminos)

Kjerfve, B., K.E. Magill, and J.E. Sneed. Modeling of circulation and dispersion in Laguna de Terminos, Campeche, Mexico. Submitted to Ecology of the Southern Gulf of Mexico with Special Reference to the Terminos Lagoon Region. A. Yáñez-Arancibia. UNAM. Mexico.

MODELING OF CIRCULATION AND DISPERSION IN LAGUNA DE TERMINOS, CAMPECHE, MEXICO[1]

Björn Kjerfve[2], K.E. Magill, and J.E. Sneed
Belle W. Baruch Institute for Marine Biology and Coastal Research
University of South Carolina
Columbia, S.C. 29208, U.S.A.

1. Contribution No. XXX from the Belle W. Baruch Institute for Marine Biology and Coastal Research.

2. Also Department of Geology and Marine Science Program, University of South Carolina.

ABSTRACT

Shallow coastal lagoons lend themselves particularly well to numerical modeling. Vertically integrated hydrodynamic and dispersion models have been applied to Laguna de Terminos, Mexico. By varying river discharge and wind stress and forcing the models with tidal harmonic constants at the two main entrances, circulation, water elevations, salinity and suspended sediment distributions have been simulated. The results are presented as tidally averaged distributions and indicate the complex residual flow patterns in the lagoon. For most conditions, the circulation shows residual transport currents entering through Puerto Real Inlet and exiting through El Carmen Inlet. The Stokes' drift is oppositely directed but of small magnitude. The residual salinity and suspended sediment distribution patterns indicate that the east and west regions of Laguna de Terminos largely act independently of each other. These model results provide an excellent tool for formulation of hypotheses but await more field data for necessary validation.

INTRODUCTION

Laguna de Terminos is Mexico's largest coastal lagoon, with an area of 2500 km^2. It is located in the state of Campeche at the base of the Yucatan Peninsula, bordering the southern Gulf of Mexico. The highly productive waters of Laguna de Terminos support Mexico's economically important and extensive marine fishery in the adjacent Bay of Campeche (Yáñez-Arancibia and Day, 1982). The lagoon is also located in close

proximity to present and proposed oil industries, and extensive petroleum exploration and drilling is now taking place in the area.

The potential impact of human activities in general, and of the oil industry in particular, increases the need for effective management of the lagoon's natural resources. An understanding of dynamic processes in the lagoon is essential for both predicting and preventing the potential dangers of industrial development on the system. Numerical circulation and dispersion modeling is a particularly useful method to investigate hydrodynamic and ecological processes in a lagoon. Numerical models, when properly calibrated and validated, can be used to predict currents, dispersion, and transport paths of sediments, nutrients, and pollutants within a lagoon.

We have developed and implemented a 2-D, vertically integrated, finite-difference estuarine circulation model (after Blumberg, 1977) and accompanying dispersion model. Both models are driven by tides, wind stress, and river discharge, and have the capacity to simulate vertically averaged longitudinal and lateral velocity patterns, tidal elevation distributions, and concentration distributions/fluxes for passive, conservative constituents. We present results from four numerical cases for which we ran the model on Laguna de Terminos. The four cases were chosen to simulate typical conditions during the different seasons.

Graham et al. (1981) and Dressler (1981) have previously implemented 2-D vertically integrated, finite element/difference hydrodynamic models on Laguna de Terminos. Whereas their models only simulate flow patterns and residual circulation, our model goes one step further by

also simulating the dispersion of dissolved/particulate conservative constituents based on the assumption of vertical homogeneity.

DESCRIPTION OF STUDY SITE

Laguna de Terminos, Campeche, is a shallow coastal lagoon with an average depth of 3 m. The tide is mixed, mainly diurnal. The amplitudes of the main diurnal and semidiurnal constituent tides are listed in Table 1. Isla del Carmen, a narrow carbonate sand barrier island, separates the lagoon from the adjacent Gulf of Mexico. Two deep tidal passes at either end of the barrier island permit exchange with the Gulf: Carmen Inlet to the west is at least 17 m deep, and Puerto Real Inlet to the east is at least 12 m deep. Three rivers discharge into the lagoon; Rio Chumpan, Rio Candelaria, and Rio Palizada. The latter is a distributary of the Usumacinta-Grijalva river system, the largest river system in Mexico and second only to the Mississippi River in the Gulf of Mexico. The Palizada provides most of the river input to the lagoon, with an estimated mean annual discharge of 500 $m^3 s^{-1}$.

The climate of this region is characterized by three distinct seasons: the wet season is from June to September, with daily afternoon and evening showers; October to February is the season of winter storms or "nortes", characterized by occasional strong northwesterly winds (8-10 m s^{-1}) with rains, particularly from November to January; and March through May is the dry season. Except during the norte season, winds are strongly influenced by the northeast trades, which locally blow predominantly from the east-southeast at 4-6 m s^{-1} (Yáñez-Arancibia and Day, 1982).

For portions of the year, Laguna de Terminos experiences distinct gradients in salinity, turbidity, and nutrients, and is from this viewpoint, a particularly interesting system in which to model circulation and dispersion patterns. During the trade wind season, there is a strong net inflow at Puerto Real Inlet, with net outflow occurring at Carmen Inlet (Gierloff-Emden, 1977). This net circulation pattern, combined with river discharge, helps to establish a persistent gradient from turbid, nutrient-rich, riverine influenced waters in the southwestern part of the lagoon near the outflow of Rio Palizada, to transparent, high salinity, marine waters in the eastern portion of the lagoon near Puerto Real Inlet (Yáñez-Arancibia and Day, 1982).

NUMERICAL MODEL FORMULATION

The hydrodynamics model selected for this study is an improved and extended version of the estuarine tidal model of Blumberg (1977). The governing equations of the model are the global shallow water equations (Welander, 1957), which result after vertical integration of the momentum balance equations. The equations are unsteady, retain the non-linear field acceleration terms, and include earth rotation, barotropic pressure gradients, wind stress, non-linear bottom friction, and horizontal diffusion of momentum. Following the notation of Blumberg (1977), integration of the x-component and y-component equations of motion yields

$$\frac{\partial uD}{\partial t} + \frac{\partial u^2D}{\partial x} + \frac{\partial uvD}{\partial y} - fvD + gD\frac{\partial \eta}{\partial y} = \tau_x^w - ku(u^2 + v^2)^{\frac{1}{2}} \qquad (1)$$

$$\frac{\partial vD}{\partial t} + \frac{\partial vuD}{\partial x} + \frac{\partial v^2D}{\partial y} + fuD + gD\frac{\partial \eta}{\partial y} = \tau_y^w - ku(u^2 + v^2)^{\frac{1}{2}} \qquad (2)$$

where u and v are the vertical averages of the depth-dependent velocities, u' and v', respectively, i.e.

$$u = \frac{1}{D} \int_{-H}^{\eta} u' \, dz; \tag{3}$$

$$v = \frac{1}{D} \int_{-H}^{\eta} v' dz \tag{4}$$

η is the surface elevation relative to mean tide; H is the water depth at mean tide level; and D is the instantaneous water depth, give by $D = H + \eta$. The Coriolis parameter, f, is expressed using the β-plane approximation

$$f = f_o + \beta \, (\Phi \pm \phi_o)R \tag{5}$$

which accounts for the change in Coriolis parameter with latitude. The northernmost latitude in the modeled system is ϕ_o, ϕ is the actual latitude, and R is the earth radius (6.37×10^6 m). The Coriolis parameter at latitude ϕ is $f = 2\Omega\sin\phi$, where $\Omega = 7.29 \times 10^{-5}$ s^{-1}. The B-factor is $2\Omega\cos\phi_o/R$; g is gravity (9.81 m s^{-2}); k is a nondimensional bottom friction factor; N is a horizontal eddy viscosity (L^2T^{-1}); and τ_x and τ_y are the x and y components of the surface wind stress, give by

$$\tau = \rho_a \, C_{10} W^2/\rho w \tag{6}$$

where ρ_a is density of air (1.2 kg m^3); ρ_w is density of estuarine water (1020 kg m^{-3}); and $C_{10}(1.6 \times 10^{-3})$ is a non-dimensional drag coefficient at 10 m elevation.

The vertically intergrated mass conservation (continuity) equation is also needed to prescribe the motion

$$\frac{\partial \eta}{\partial t} + \frac{\partial uD}{\partial x} + \frac{\partial vD}{\partial y} = 0 \qquad (7)$$

The above formulation of the governing equations assumes that the water is homogeneous and incompressible, and that longitudinal pressure gradients due to density variations are neglible (cf. Blumberg, 1978). By integrating the equations vertically, information about the vertical velocity structure is lost. However, for a shallow, well-mixed water column such as in Laguna de Terminos, this is not a serious shortcoming. Information about dispersion of pollutants is essentially retained when the local velocity, i.e. the velocity found at any specified depth, is well approximated by the global velocity, i.e. the velocity averaged over the water column. This approximation is generally valid in shallow, well-mixed waters.

Analytic solutions to the non-linear global equations with realistic boundary conditions are not possible. However, numerical integration of the equations is possible on a digital computer. The non-linear set of governing partial differential equations is therefore expressed as finite difference equations, and solved explicitly by the method described by Blumberg (1977). The finite difference equations are second order accurate in space and first order in time. All finite difference modeling was carried out on a Digital VAX 11/780 mainframe computer at the University of South Carolina.

Using the notation of Blumberg (1977), the linear difference operators for average and second order differencing, respectively, are

$$\overline{F(x,y,t)}^{x} = \frac{F(x + \frac{\Delta x}{z},y,t) + F(x - \frac{\Delta x}{z},y,t)}{2} \tag{8}$$

$$\delta_x[F(x,y,t)] = \frac{F(x + \frac{\Delta x}{z},y,t) - F(x - \frac{\Delta x}{z},y,t)}{\Delta x} \tag{9}$$

The global equations in second order finite difference form are given by

$$\frac{(\bar{D}^{x} u)^{n+1} - (\bar{D}^{x} u)^{n-1}}{2\Delta t} + \delta_x(\overline{\bar{D}^{x} u}^{x} \bar{u}^{x}) + \delta_y(\overline{\bar{D}^{x} v}^{y} \bar{u}^{y}) -$$

$$f\overline{\bar{D}^{x} v}^{xy} = g\bar{D}^{x}\delta_x\eta - \tau_x + k[u(u^2 + \overline{\bar{v}^{xy}}^{2})^{\frac{1}{2}}]^{n-1} = 0 \tag{10}$$

$$\frac{(\bar{D}^{y} v)^{n+1} - (\bar{D}^{y} v)^{n-1}}{2\Delta t} + \delta_x(\overline{\bar{D}^{y} u}^{x} \bar{v}^{x}) + \delta y(\overline{\bar{D}^{y} v}^{y} \bar{v}^{y}) -$$

$$f\overline{\bar{D}^{y} u}^{xy} + g\bar{D}^{y}\delta_x\eta - \tau_y^{w} + k[v(\overline{\bar{u}^{xy}}^{2} + v^2)^{\frac{1}{2}}]^{n-1} = 0 \tag{11}$$

$$\frac{\eta^{n-1} - \eta^{n-1}}{2\Delta t} + \delta_x(\bar{D}^{x} u) + \delta_y(\bar{D}^{y} v) = 0 \tag{12}$$

where the superscript n refers to time level.

The model is forced by prescribed tidal constituent amplitudes and phases at the open ocean boundary, wind stress over the lagoon, and freshwater input from the three rivers. Numerical integration is carried out by taking an initial forward step in time at the open boundary, solving for η (eq. 7), and then for the u and v components (eqs. 1 and 2). This leap-frog integration scheme is then repeated for all elements until simulation is completed.

To obtain numerical simplicity, the u and v components and η are calculated for different positions within each grid, similar to Blumberg (1977). The H, D, and η values are specified at the middle of each grid. The v components are calculated for points $\Delta y/2$ north and south of the mid point, including any east-west boundary, and the u components are calculated for points $\Delta x/2$ east and west of the mid point, including any north-south boundary (Blumberg, 1977). The condition of no normal flow through a land boundary is easily satisfied with this off-set computational scheme. It also has the added advantage that central difference approximations to derivatives of the off-set variables involve points only one grid-length apart.

The computational time step, Δt, mut be smaller than a critical time step

$$\Delta t < \tfrac{1}{2}[(gD_{max})^{\frac{1}{2}} (1/\Delta x + 1/\Delta y)/2]^{-1} \qquad (13)$$

for the numerical solution.

Blumberg (1977) and Tee (1976) found that any simplifications of the governing equations produced major changes in the simulated circulation patterns. Similarly, we found that simplified equations produced significantly altered circulation patterns. Thus, inclusion of all the terms in equations 1 and 2 is necessary to produce a realistic circulation model. Our choice for the friction factor was k = 0.0025. The wind stress was varied to allow for different wind stresses.

Once the global water level and velocity fields have been simulated for the lagoon, the advection and dispersion of a passive conservative constituent, c, can be determined. The governing equation is the distribution of variables equation

$$\frac{\partial cD}{\partial t} + \frac{\partial uDc}{\partial x} + \frac{\partial vDc}{\partial y} = \frac{\partial}{\partial x}(DK_x \frac{\partial c}{\partial x}) + \frac{\partial}{\partial y}(DK_y \frac{\partial c}{\partial y}) + F_\eta(x,y,\eta) - F_H(x,y,-H) \quad (14)$$

where the F's are the vertical fluxes of a constituent at the surface and at the bottom, K_x and K_y are horizontal eddy diffusivities, and C is the constituent concentration.

Non conservative substances would require inclusion of a vertically integrated source-sink term, S(x,y), in the equation. The finite difference form of the advection-dispersion relationship is

$$\frac{(DC)^{n+1} - (DC)^{n-1}}{2\Delta t} + \delta_{\overline{x}}^{x}(\bar{D}^{n} u_x c) + \delta_{\overline{y}}^{x}(\bar{D}^{n} v_y c) = \delta_x(\bar{D}^{x} K_x \delta_x c)^{n-1} + \delta_y(\bar{D}^{y} K_y \delta_y c)^{n-1} + F_\eta + F_{-H} + S \quad (15)$$

In addition to the surface and bottom fluxes of substance c, values of c on lateral boundaries are required for water advected into the lagoon, whether it be from the ocean or from the rivers.

The equations, as formulated, neglect lateral friction but include lateral eddy diffusion. This apparent inconsistency is due to the fact that surface and bottom friction dominate over lateral friction in the momentum equation, but there is no mechanism other than horizontal diffusion to mix waters advected with the velocity field. The horizontal mixing, in reality, is partly achieved by the apparent spreading of a water mass due to the combined effect of vertical diffusion and vertical shear of the local horizontal velocity. This effect cannot be directly

represented in the global equation model. However, it can be empirically parameterized by horizontal diffusion.

The numerical formulations which we have used are best suited to simulate water level changes, velocity fields, and constituent dispersion in shallow coastal lagoons, which are well-mixed vertically.

Blumberg's (1977) numerical algorithm was found to have several shortcomings: 1) the divergence of momentum flux, water flux, and substance flux involved repetitious calculation of fluxes; 2) the relation between the grid, variable storage, and boundary conditions did not lend itself to altering boundary conditions or dynamics; and 3) the divergence of substance flux gave rise to artifacts (the Gibbs effect) in the vicinity of sharp gradients.

We have made the following improvements to the model: 1) all model values are referenced to a single, unique grid; 2) repetitive flux calculations have been eliminated by storing previously calculated fluxes; 3) boundary conditions have been implemented in a direct and flexible manner; 4) the model has been modularized to improve readability and ease any further extension ; and 5) the leap frog scheme for advection, used by Blumberg, has been replaced by a flux corrected transport (FCT) system (Boris and Book, 1973; Zalesak, 1979) in order to eliminate the Gibbs effect near sharp gradients.

IMPLEMENTATION OF MODEL

The model was implemented using a 54 row by 21 column grid, with each element measuring 1200 m X 1200 m (Fig. 1). Water depths in the grid range from 1-4 m, which allowed for the use of a 60 second time

step (eq. 13) for all model runs. The model is driven by simulated tides at Puerto Real and Carmen Inlet, a specified uniform wind field over the entire model domain, and river discharges for the Chumpan, Candelaria, and Palizada rivers.

Output from the model consists of several graphic products. Nine residual plots, computed over any desired averaging period [we chose to average over 1 diurnal tidal cycle (24.84 hrs.)] may be output. These include plots of water elevations, salinities, and suspended sediments, presented as contour plots which are normalized to a [0,1] range by

$$\zeta = [C(x,y,t) - C_{min}] \; / \; [C_{max} - C_{min}] \qquad (16)$$

where ξ is the contour interval; C(x,y,t) is the computed value at a specified grid element (x,y); C_{min} is the minimum value of the variable found in the grid; and C_{max} is the maximum value of the variable. We also produced vectoral water velocity plots presented as either net (average) velocities, Stoke's (depth-weighted) velocities, or langrangian velocities (the difference between the net and Stoke's). Each of the three velocity representations may be plotted with either dimensional point vectors or non-dimensional streamlines. Also, instantaneous values of water elevation, salinity, suspended sediments, and velocity may be plotted for any specified time interval. In all of our modeled cases we chose to plot instantaneous values every 3 lunar hours.

In addition, time series of salinity, suspended sediments, water elevation, and water velocity may be created at any number of specified grid points and at any desired sampling rate. For each case modeled, we created time series every 0.25 lunar hour from 6 points within the grid.

Using the time series data from each specified point, we could then generate: 1) progressive vector diagrams; 2) wind speed and direction roses; and 3) time series plots of currents, salinity, suspended sediments, and water elevations.

To determine how long it took the models to reach steady state, we implemented a cold-start 28-tidal cycle run which simulated trade wind conditions (Table 2), mean river discharge, and the tidal constituents given in Table 1. We found that the hydrodynamic model reaches steady state relatively quickly, after only 2-3 diurnal tidal cycles. However, steady state conditions in the dispersion model were met only after 14 tidal cycles. All subsequent runs were therefore hot-started from the 14th tidal cycle of this initial run, and then run for an additional 14 tidal cycles.

Four separate cases were modeled in this study. The input values for each case were chosen to simulate the range of climatic conditions which are encountered during each of the three seasons (Table 2). The first case, as previously mentioned, was run for 28 tidal cycles, and simulated homogeneous trade winds over the entire lagoon and mean river discharge from the three rivers. This case represents the dry season during spring. Initial input values of salinity and suspended sediments at the inlets and rivers are given in Table 2. The second case simulated mean river discharge with no winds, and represents the transition from the dry to the wet season in early-mid summer. The third case simulated "norte" winds with mean river discharge, and reflects the season of "nortes" in late autumn - early winter. Finally, case 4 simulated flood conditions with peak discharge and no winds. This case is representative

of the wet season in late summer - early autumn.

In all four cases, the tidal constituents used as inputs to the model (Table 1) were held constant. They were derived through harmonic analysis at each inlet, and reflect a mixed, mainly diurnal tide regime, with the tides at Carmen Inlet leading those at Puerto Real Inlet by one hour.

RESULTS

In case 1, water level setup is clearly forced by the trade winds. Residual water elevation contours (Fig. 2a) are oriented normal to the local east-southeasterly trade wind direction. Elevations range from 0.38 m at the extreme east side to 0.40 m near Carmen Inlet. Tidally-averaged salinities (Fig. 2b) range from a minimum of 4.5 ppt near the Palizada river mouth to 34.5 ppt at the mouth of Puerto Real Inlet. Salinities are high in the central portion of the lagoon due to the input of 35 ppt salinity water through Puerto Real Inlet, and decrease significantly near the mouth of the Palizada River. The tidally-averaged suspended sediment profile (Fig. 2b) is inverse to that of the salinity field. Maximum suspended sediment concentrations of 89 ppm occur at the Palizada mouth, while concentrations to the east of the Palizada decrease rapidly to less than 27 ppm. The depth-averaged residual circulation (Fig. 3), shows a predominant westward flow in through Puerto Real and out at Carmen Inlet. Graham et al. (1981) and Dressler (1981) produced similar net westward flow patterns with their models. The streamline plot of the depth-averaged residual circulation (Fig. 3b) emphasizes several eddies which have formed in the lagoon.

In case 2, there is insignificant water level setup in the lagoon. An increase in water elevations occurs going into the mouth of Puerto Real, but the rest of the lagoon maintains a nearly uniform water level (Fig. 4a). The rivers, in particular the Palizada, greatly influence the circulation and dispersion in the lagoon. Salinities (Fig. 4b) range from 2.5 ppt near the Palizada river mouth to 34.5 ppt near Puerto Real Inlet. Again, suspended sediments (Fig. 4c) display a strong inverse relationship to salinities, with 20 ppm concentrations near Puerto Real Inlet and a maximum of 94 ppm near the Palizada mouth. The residual circulation (Fig. 5), shows strong currents flowing out of the rivers, particularly the Palizada, with export of waters occurring through both inlets. With the exception of the Palizada river mouth and the two inlets, current velocities are very weak throughout the lagoon. The streamline plot (Fig.5b) is more useful than the vectoral plot (Fig. 5a) for depicting the residual circulation when currents are weak as in this case.

In case 3, water level setup appears to be forced by the norte wind regime, as elevation contours are oriented normal to the wind direction (Fig. 6a). A maximum water elevation of 0.51 m is found to the extreme south, while a minimum of 0.39 m is located near the extreme northern edge. The minimum salinity of 8.3 ppt (Fig. 6b) is considerably higher than the minimum for the other two cases. Likewise, the maximum suspended sediment concentration of 80 ppm (Fig. 6c) is slightly lower than for the first two cases. Norte winds appear to be the dominant force in controlling dispersion in the model, while the effect of the rivers is largely suppressed. The direction of river flow generally opposes the stronger wind induced currents. Residual current velocities (Fig. 7)

are much stronger than in the first two cases, with maximum velocities reaching 17.0 cm/s. Residual circulation patterns are also more complex in this case. There is a strong southward flow, apparently wind-induced, along the east and west sides of the lagoon. The river flow has also set up opposing currents which appear to have generated a series of anticyclonic eddies in the eastern half of the lagoon and cyclonic eddies in the western half. The streamline plot (Fig. 7b) is particularly useful in emphasizing the location of these eddies and fronts.

The water level setup in case 4 (Fig. 8a) is very similar to that in case 2 except that the slope is greater. Elevations cover a 3.5 cm range. Water level is highest in the extreme southern portion of the lagoon and lowest at Puerto Real Inlet. The higher water levels are presumably due to the tremendous increase in river discharge, from 300 to 2000 $m^3 s^{-1}$ for the Rio Palizada. Minimum salinities (Fig. 8b) of 0.1 ppt are found near the Palizada mouth and maximum salinities of 33 ppt occur in the eastern part of the lagoon. This is the largest salinity range of all cases. Suspended sediment concentrations and gradients are also maximum in this case (Fig. 8c), ranging from 23 ppm to 173 ppm. The gradient is in the opposite direction to that of salinity, pointing westward with a low in the eastern portion of the lagoon. Maximum currents of 30 cm s^{-1} are reached near the mouth of the Rio Palizada, and the depth-averaged residual circulation (Fig. 9) shows an export out of the lagoon via both inlets. River flow is clearly the major force influencing circulation and dispersion in this case.

FINAL COMMENTS

The results from our four simulation runs show that tides, freshwater discharge, and local winds are all major forcing mechanisms of circulation and dispersion in Laguna de Terminos. Our results are preliminary and validation of the model has yet to be performed. Still, the simulation runs are important and useful in several respects. They represent conditions that may exist under realistic environmental situations, i.e. actual seasonal wind regimes, river discharge conditions, and tidal constituents at the two inlets. In carrying this project one step further, field sampling schemes will be developed in order to provide verification for the model results. Our four model simulations will prove useful in choosing the best location and optimum number of sampling sites for existing season/weather conditions. The hydrodynamic/dispersion simulations are a particularly important resource to use in formulating hypotheses.

REFERENCES

Blumberg, A. 1977. Numerical tidal model of Chesapeake Bay. Journal of the Hydraulics Division, Proceedings of the ASCE, 103 (HYI): 1-10.

Boris, J.P. and D.L. Book. 1973. Flux-corrected transport I: SHASTA. A fluid transport algorithm that works. J. Physics 11:38-69.

Day, J.W., R.H. Day, M.T. Barreiro, F. Ley-Lou, and C.J. Madden. 1982. Primary production in the Laguna de Terminos, a tropical estuary in the southern Gulf of Mexico. Oceanológica Acta. Volume Spécial: 269-276.

Dressler, R. 1981. Investigación sobre mareas y efectos del viento en la Laguna de Terminos (Mexico) - mediante un modelo hidrodinámico-numerico. Informe Tecnicio. CICESE: OC 82:01. Esenada, Baja California, Mexico. 36 pp.

Gierloff-Emden, H.G. 1977. Laguna de Terminos and Campeche Bay, Gulf of Mexico: water mass interaction lagoonal oceanic visible due to sediment laden waters, pp. 77-89. In: Orbital remote sensing of coastal and offshore environments, a manual of interpretation. Walter de Gryter (ed.), Berlin.

Graham, D.S., J.P. Daniels, J.M. Hill, and J.W. Day. 1981. A preliminary model of the circulation of Laguna de Terminos, Campeche, Mexico. An. Inst. Cienc. del Mar y Limnol. Univ. Nal. Autón, México. 8:51-62.

Welander, P. 1957. Wind action on a shallow sea: some generalizations of Ekman's theory. Tellus 9:45-52.

Yáñez-Arancibia, A. and J.W. Day, Jr. 1982. Ecological characterization of Terminos Lagoon, a tropical lagoon-estuarine system in the Southern Gulf of Mexico. Oceanológica Acta. Volume Spécial: 431-440.

Zalesak, S.T. 1979. Fully multidimensional flux-corrected transport algorithm for fluids. J. Physics 31:335-362.

CAPTIONS

Fig. 1. (a) Bathymetry used to implement model on Laguna de Terminos, Campeche, Mexico. The model used a 54 x 21 element grid with elements measuring 1200 x 1200 m. The model is driven by simulated tides at the two inlets, a specified uniform wind field, and river discharge at the three river mouths designated by "arrows". The "triangle" symbols specify 6 points at which time series are developed for calibration and validation purposes. (b) Grey-scale representation of bathymetric contours.

Fig. 2. Case 1 (simulated trade winds; mean river discharge; mixed mainly diurnal tides): (a) Tidally-averaged net water elevations, (b) salinity concentrations, and (c) suspended sediment concentrations, averaged over the 28th tidal cycle. Normalized contours 0.1 - 0.9 indicate water elevationsof 0.38 m - 0.40 m; salinity concentra tions of 7.5 - 31.5 ppt; and suspended sediment concentrations of 26.9 ppm - 82.1 ppm.

Fig. 3. Case 1 (simulated trade winds; mean river discharge, mixed, mainly diurnal tides): (a) Vectoral and (b) non-dimensional depth-averaged (Stoke's) residual circulation averaged over the 28th tidal cycle.

Fig. 4. Case 2 (no winds; mean river discharge; mixed, mainly diurnal tides): (a) Tidally-averaged net water elevations, (b) salinity concentrations, and (c) suspended sediment concentrations, averaged over the 28th tidal cycle. Normalized contours 0.1 - 0.9 represent water elevationsof 0.38 m - 0.40 m; salinity concentrations of 5.7 ppt - 31.3 ppt; and suspended sediment concentrations of 27.4 ppm - 86.6 ppm.

Fig. 5. Case 2 (no winds; mean river discharge; mixed, mainly diurnal tides): (a) Vectoral and (b) non-dimensional streamline representations of the depth-averaged (Stoke's) residual circulation averaged over the 28th tidal cycle.

Fig. 6. Case 3 (simulated norte winds; mean river discharge; mixed, mainly diurnal tides): (a) Tidally-averaged net water elevations, (b) salinity concentrations, and (c) suspended sediment concentrations, averaged over the 28th tidal cycle. Normalized contours 0.1 - 0.9 represent water elevations of 0.4 m - 0.5 m; salinity concentrations of 10.9 ppt - 31.7 ppt; and suspended sediment concentrations of 26 ppm - 74 ppm.

Fig. 7. Case 3 (norte winds; mean river discharge; mixed, mainly diurnal tides): (a) Vectoral and (b) non-dimensional streamline representations of the depth-averaged (Stoke's) residual circulation averaged over the 28th tidal cycle.

Fig. 8. Case 4 (no winds; maximum discharge; mixed, mainly diurnal tides): (a) Tidally-averaged net water elevations, (b) salinity concentra-

tions, and (c) suspended sediment concentrations, averaged over the 28th tidal cycle. Normalized water elevation contours 0.1-0.9 indicate heights of 0.38 m - 0.41 m; salinity concentrations of 3.3 ppt - 29.7 ppt; and suspended sediment concentrations of 38 ppm - 158 ppm.

Fig. 9. Case 4 (no winds; maximum discharge; mixed, mainly diurnal tides): (a) Vectoral and (b) non-dimensional streamline representations of the depth-averaged (Stoke's) residual circulation averaged over the 28th tidal cycle.

Table 1. Tidal input parameters for the four simulation runs on Laguna de Terminos

	Amplitude (m)	Phase (^{o}G)	Node Factor	Equilibrium Argument	Period (hrs)
CARMEN INLET					
K_1	0.119	317.0	1.104	6.9	23.93
O_1	0.115	318.0	1.168	232.6	25.82
M_2	0.076	082.8	0.967	238.1	12.42
S_2	0.020	021.0	1.000	0.0	12.00
PUERTO REAL INLET					
K_1	0.120	288.4	1.104	6.9	23.93
O_1	0.138	289.7	1.168	232.6	25.82
M_2	0.111	037.2	0.967	238.1	12.42
S_2	0.018	011.3	1.000	0.0	12.00

Table 2. Boundary and initial conditions on the five simulation runs. Run 1 corresponds to trade wind conditions, run 2 to no-wind conditions, run 3 to Norte conditions, and run 4 to high-runoff conditions.

	Run 1	Run 2	Run 3	Run 4
Rio Palisades				
Flow (m^3/s)	300	300	300	2000
TSS (ppm)	300	300	300	500
Salinity (ppt)	0	0	0	0
Rio Chumpan				
Flow (m^3/s)	10	10	10	30
TSS (ppm)	100	100	100	200
Salinity (ppt)	0	0	0	0
Rio Candelaria				
Flow (m^3/s)	35	35	35	80
TSS (ppm)	100	100	100	200
Salinity (ppt)	0	0	0	0
Carmen Inlet				
TSS (ppm)	30	30	30	60
Salinity (ppt)	32	32	32	20
Puerto Real Inlet				
TSS (ppm)	20	20	20	30
Salinity (ppt)	35	35	35	30
Homogeneous Wind Field				
Wind direction (^{o}from)	105	-	345	-
Wind speed (m/s)	4	0	10	0
Tidal cycles simulated	1-28	15-28	15-28	15-28

ORIGINAL PAGE IS
OF POOR QUALITY

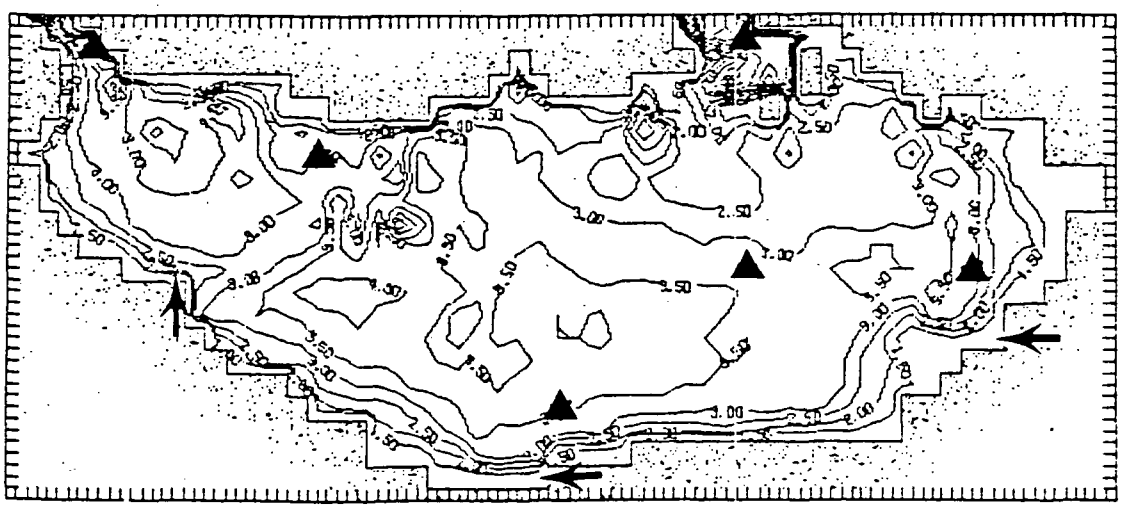

Fig. 1a

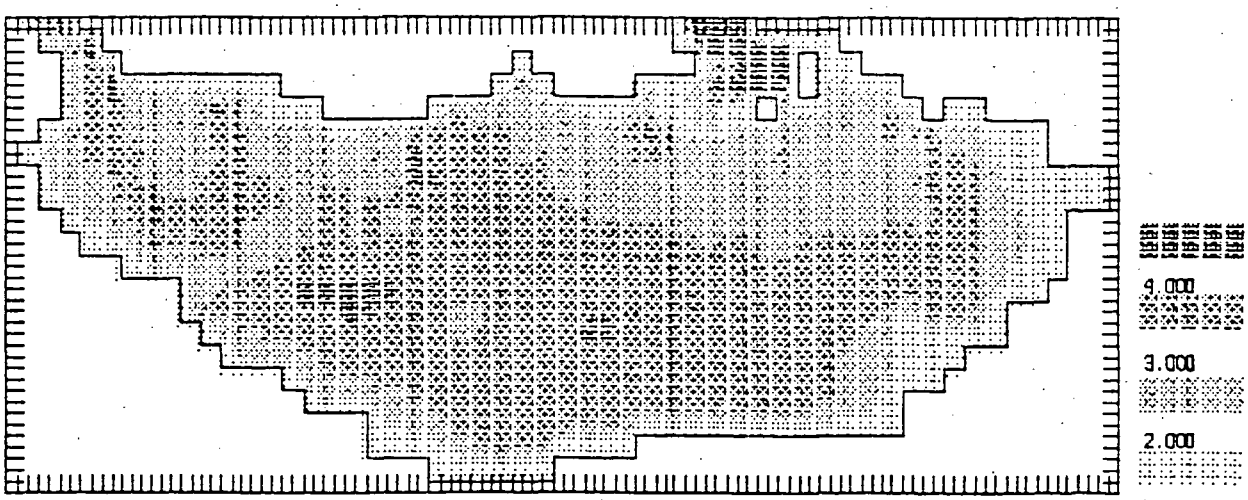

Fig. 1b

ORIGINAL PAGE IS
OF POOR QUALITY

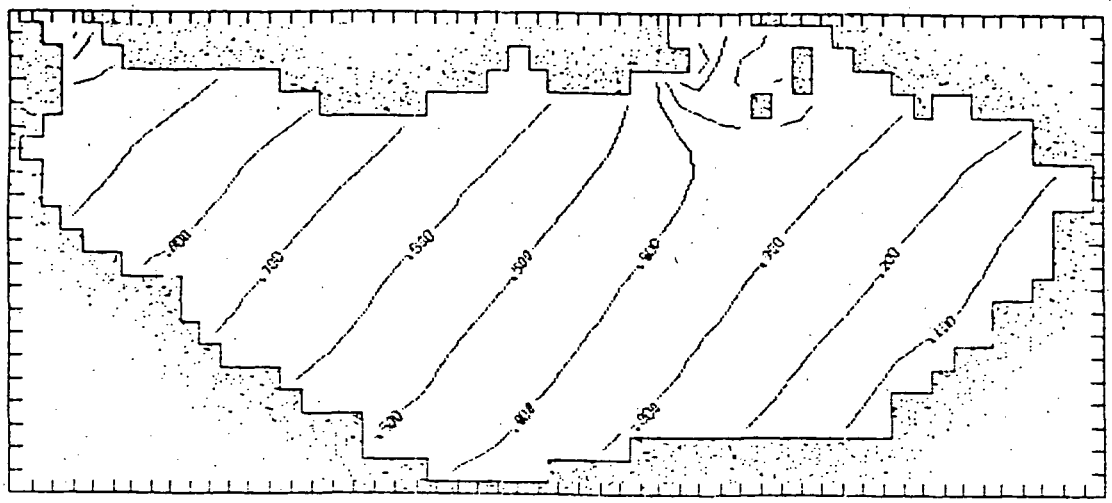

Fig. 2a

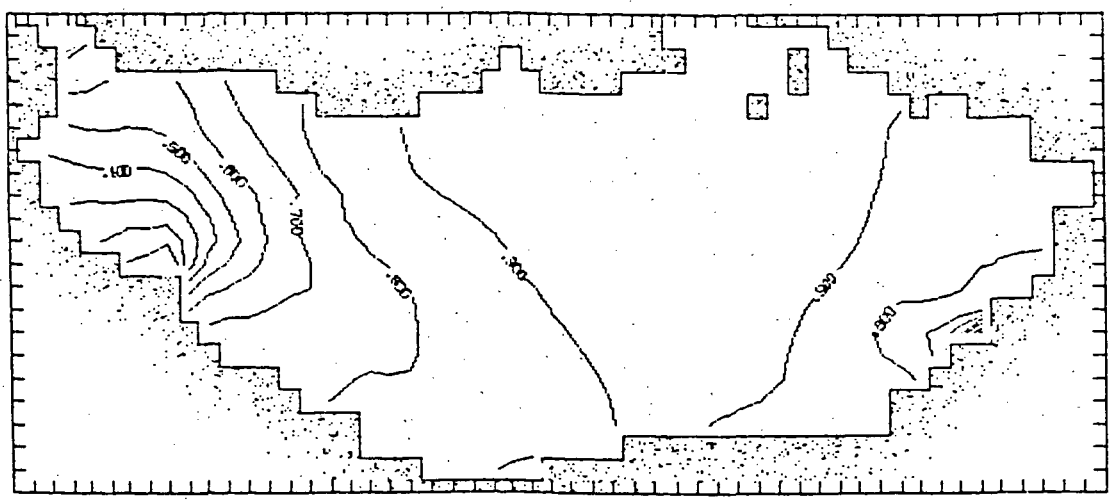

Fig. 2b

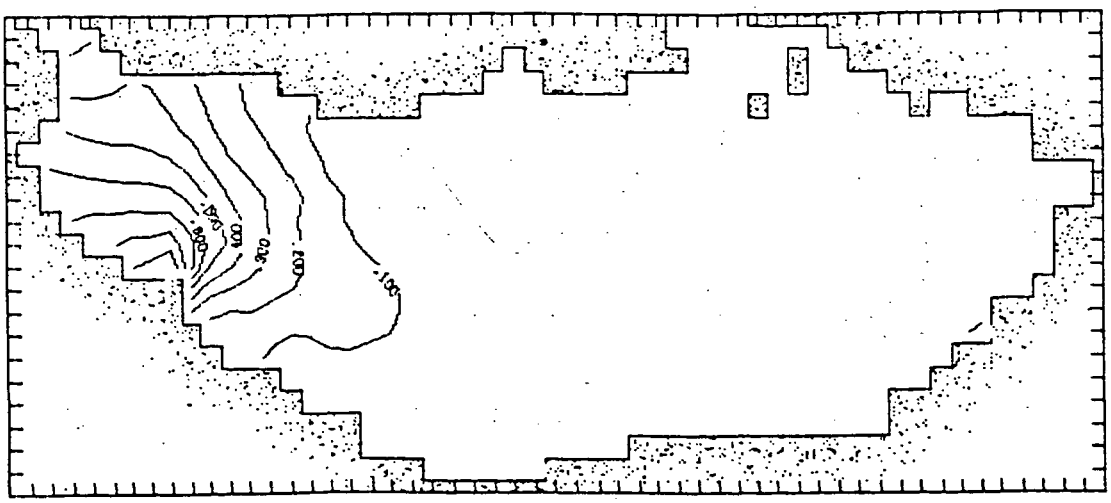

Fig. 2c

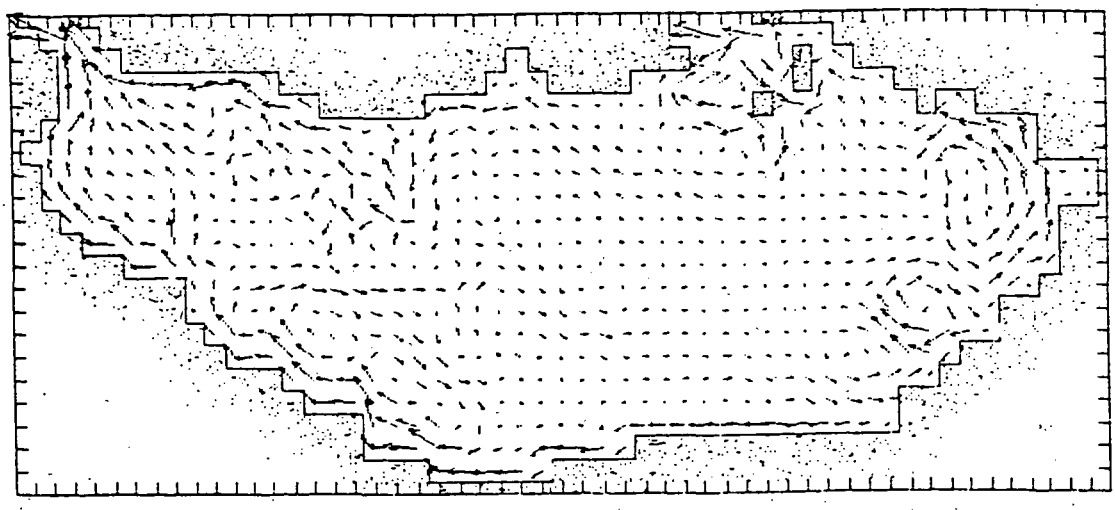

Fig. 3a

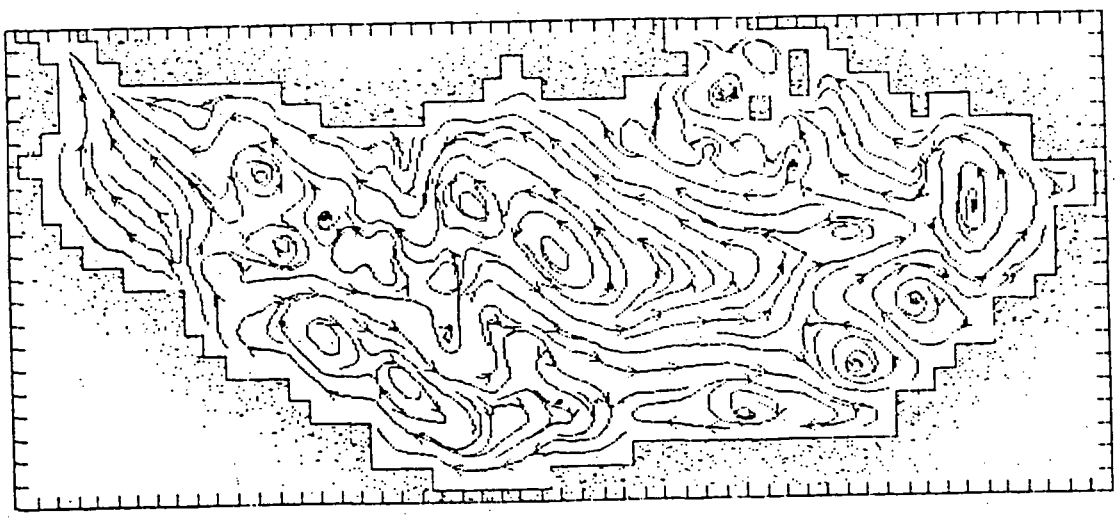

Fig. 3b

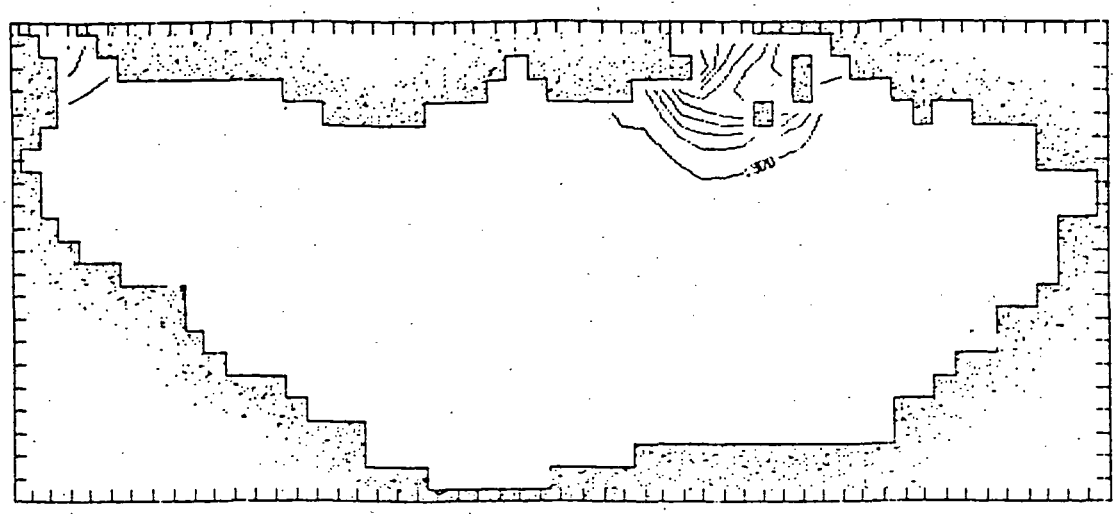

Fig. 4a

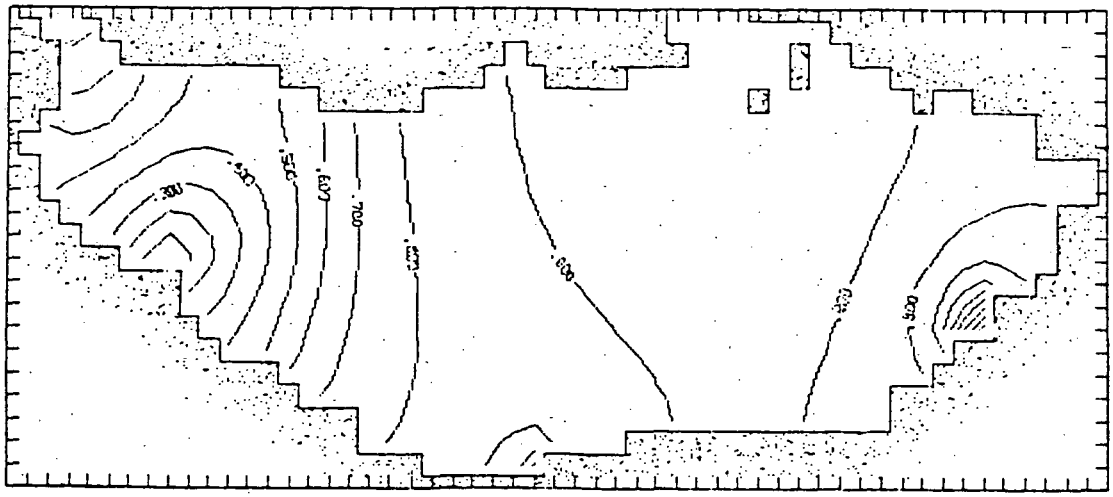

Fig. 4b

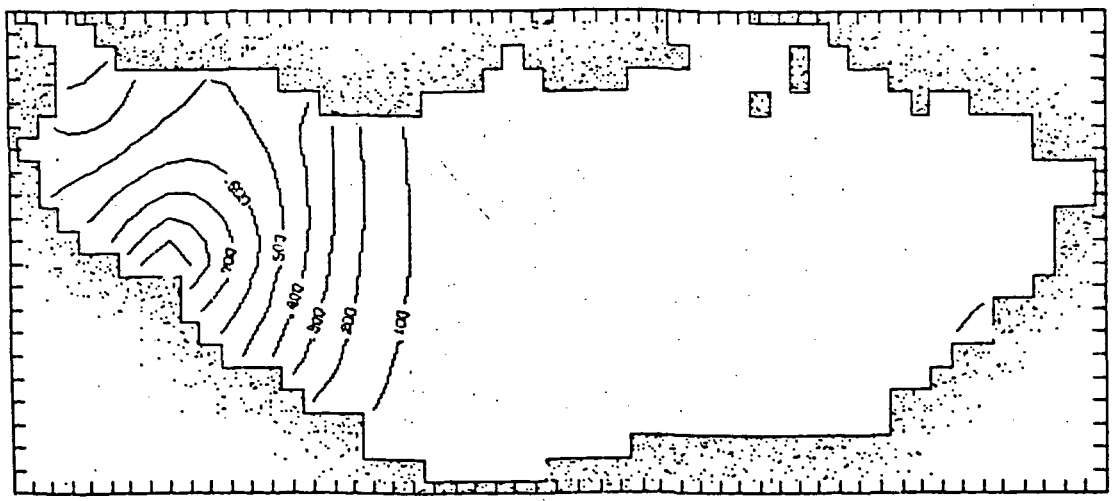

Fig. 4c

ORIGINAL PAGE IS
OF POOR QUALITY

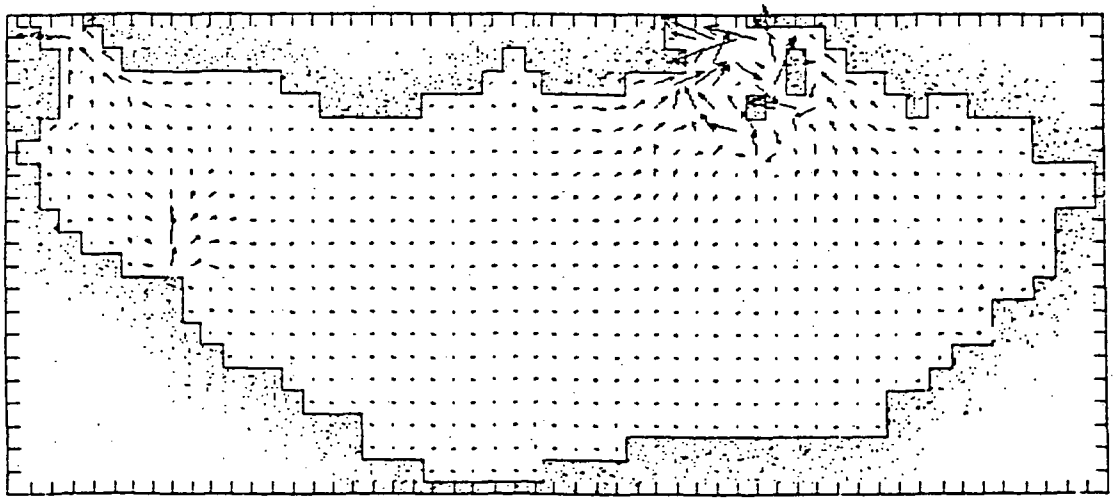

Fig. 5a

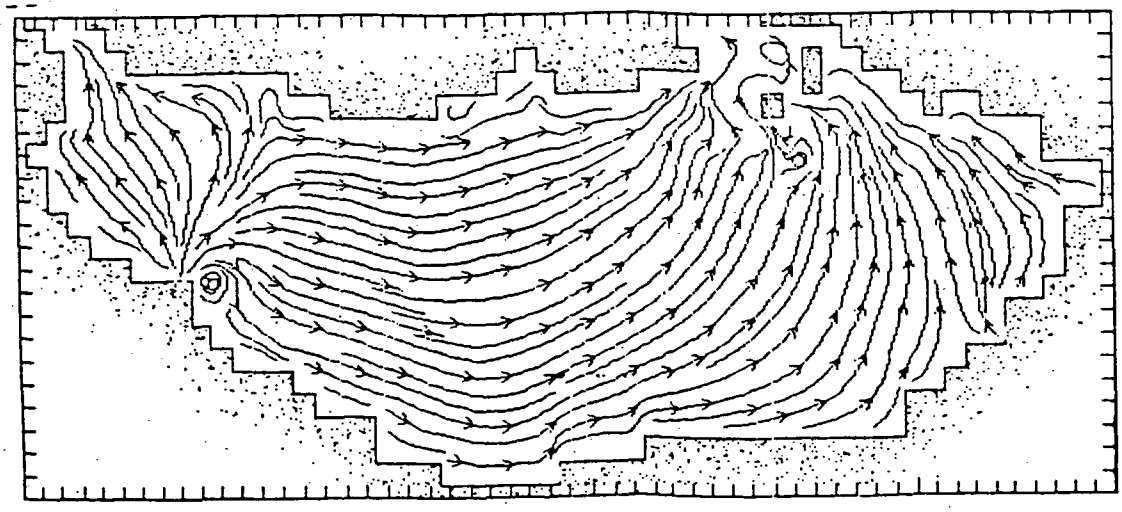

Fig. 5b

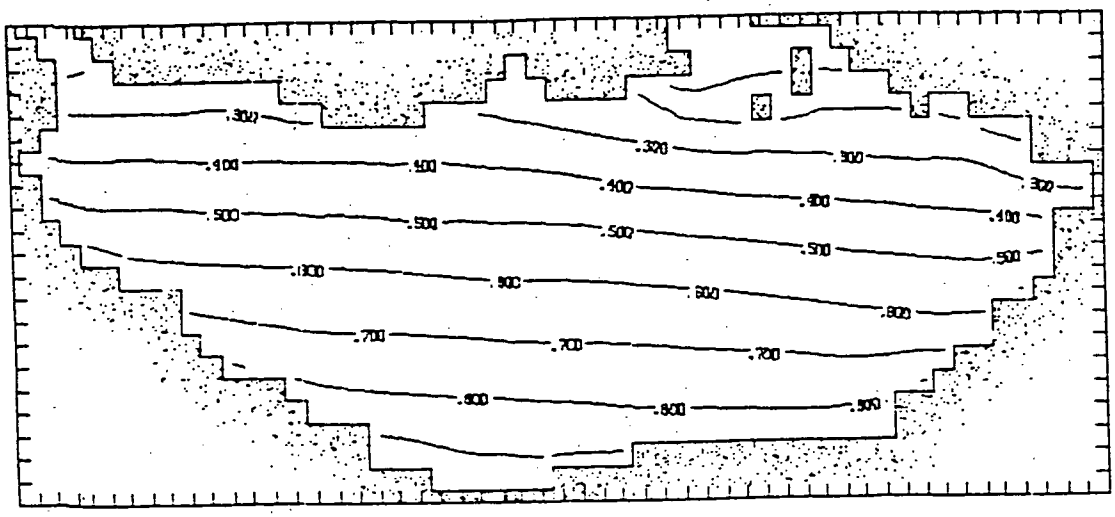

Fig. 6a

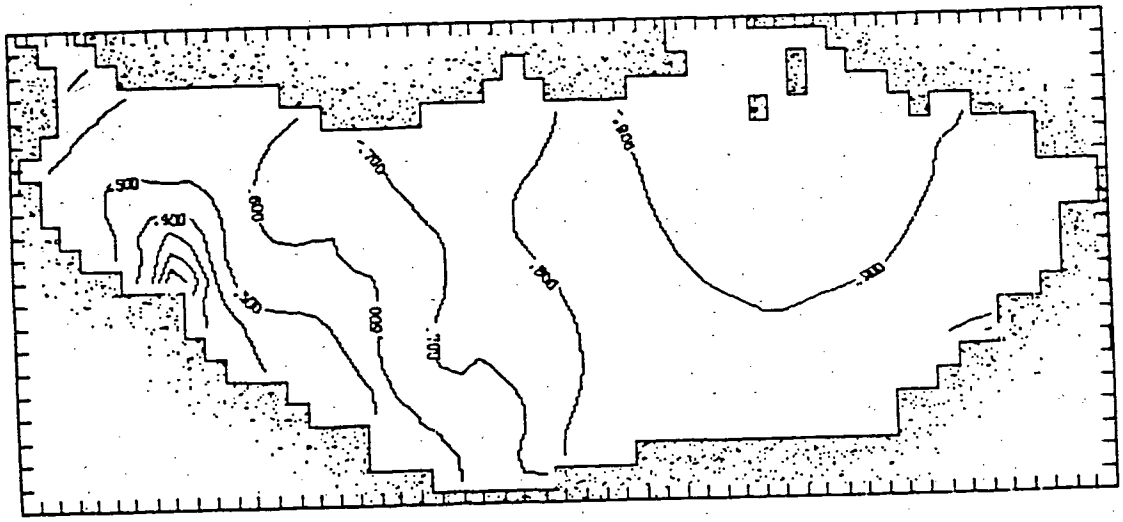

Fig. 6b

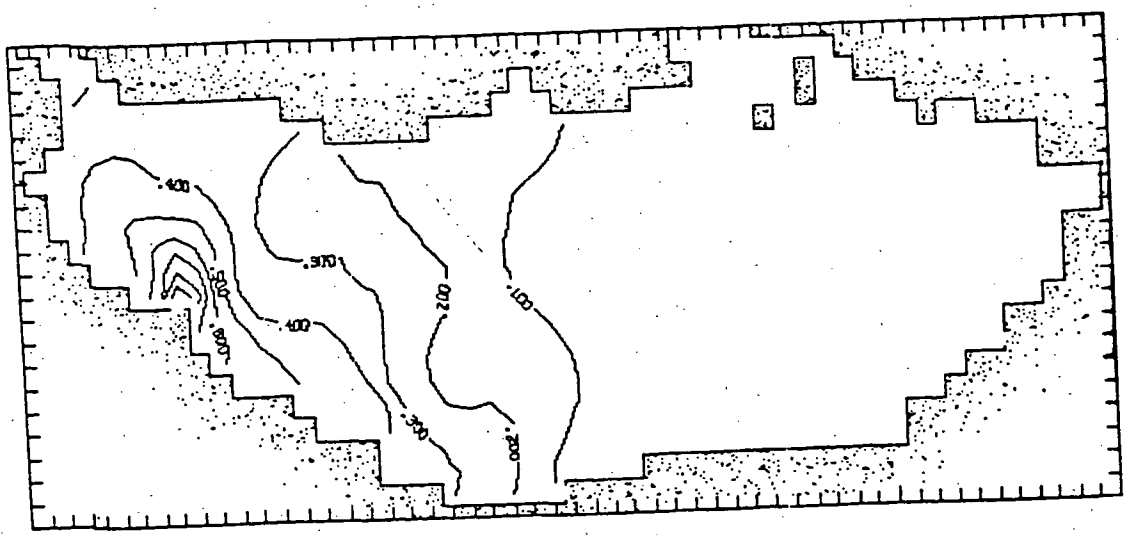

Fig. 6c

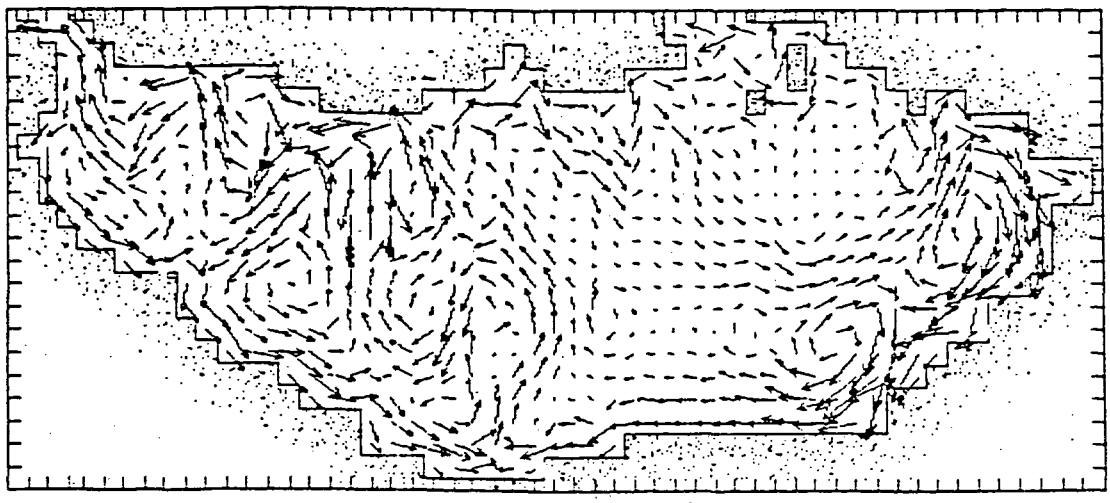

Fig. 7a

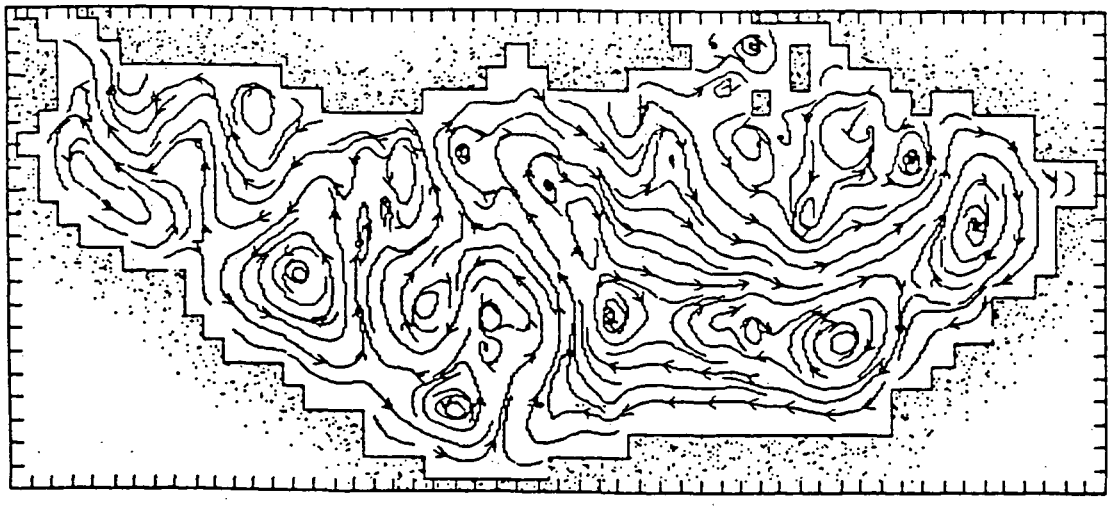

Fig. 7b

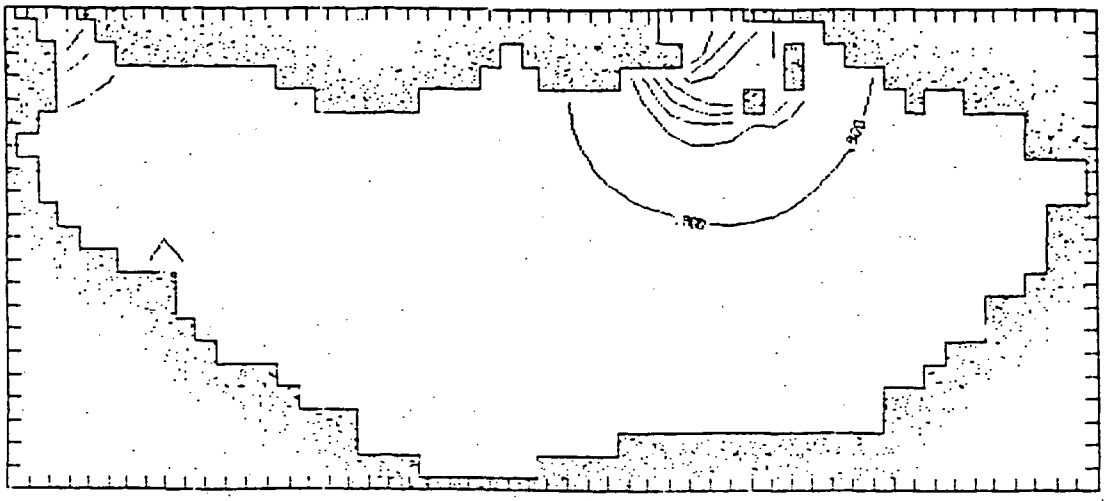

Fig. 8a

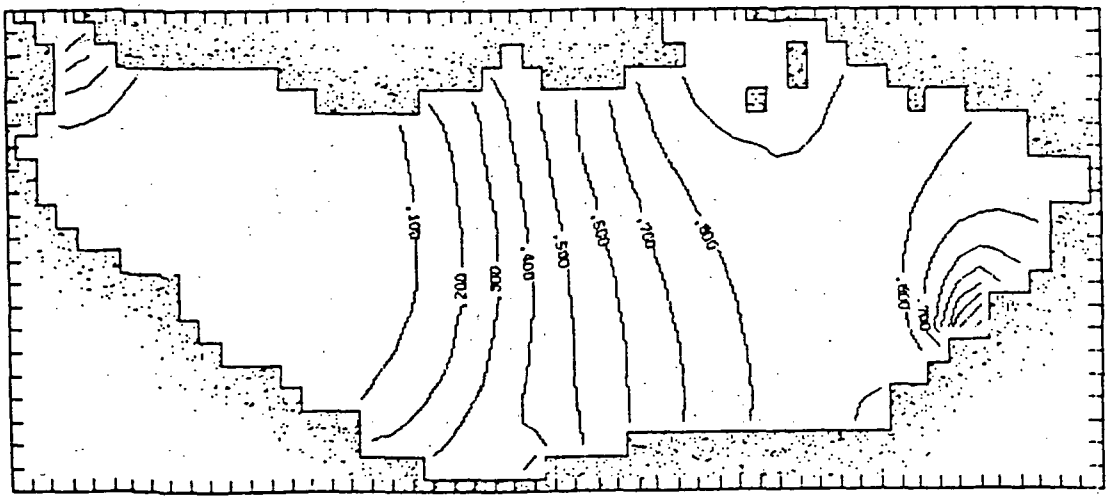

Fig. 8b

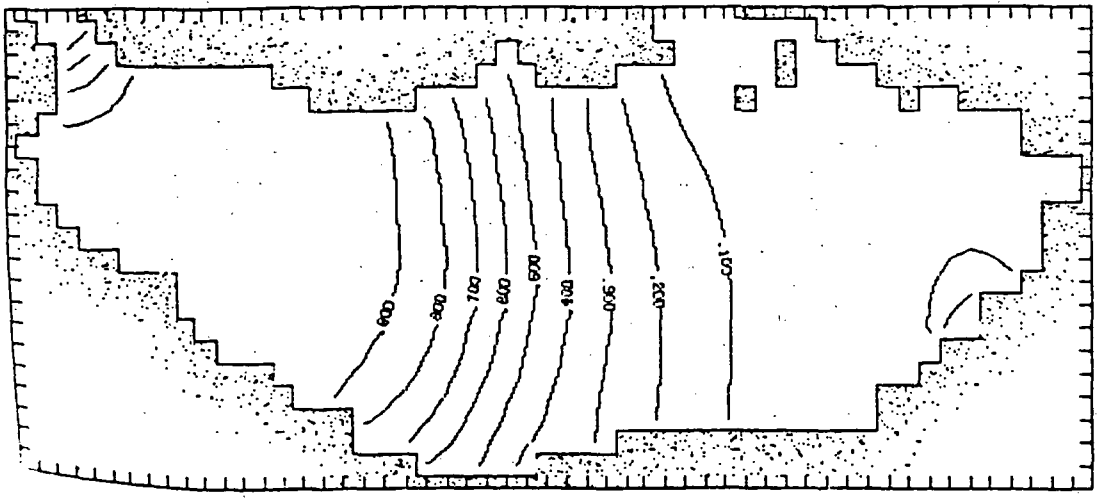

Fig. 8c

ORIGINAL PAGE IS
OF POOR QUALITY

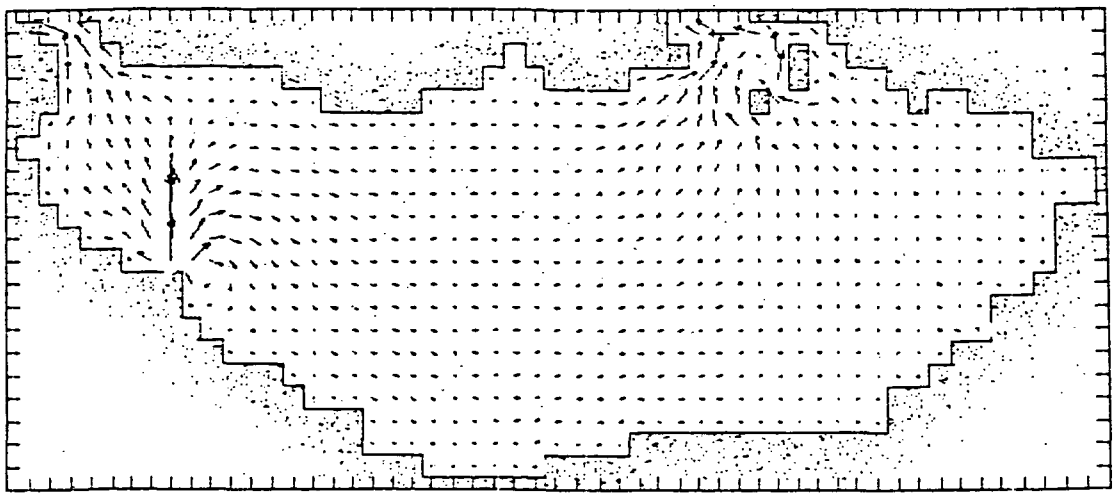

Fig. 9a

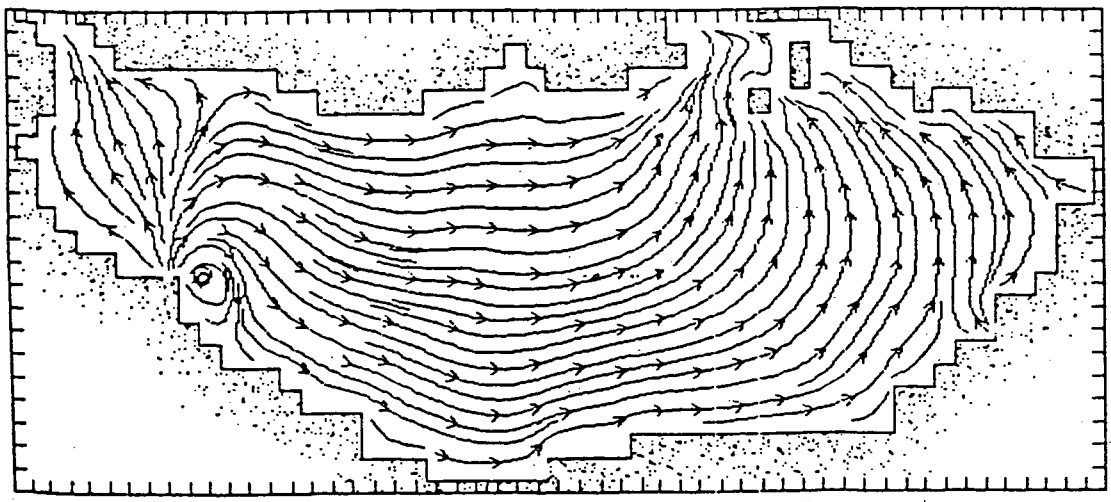

Fig. 9b

APPENDIX II

(Modeling sample graphics output from Lake Calcasieu)

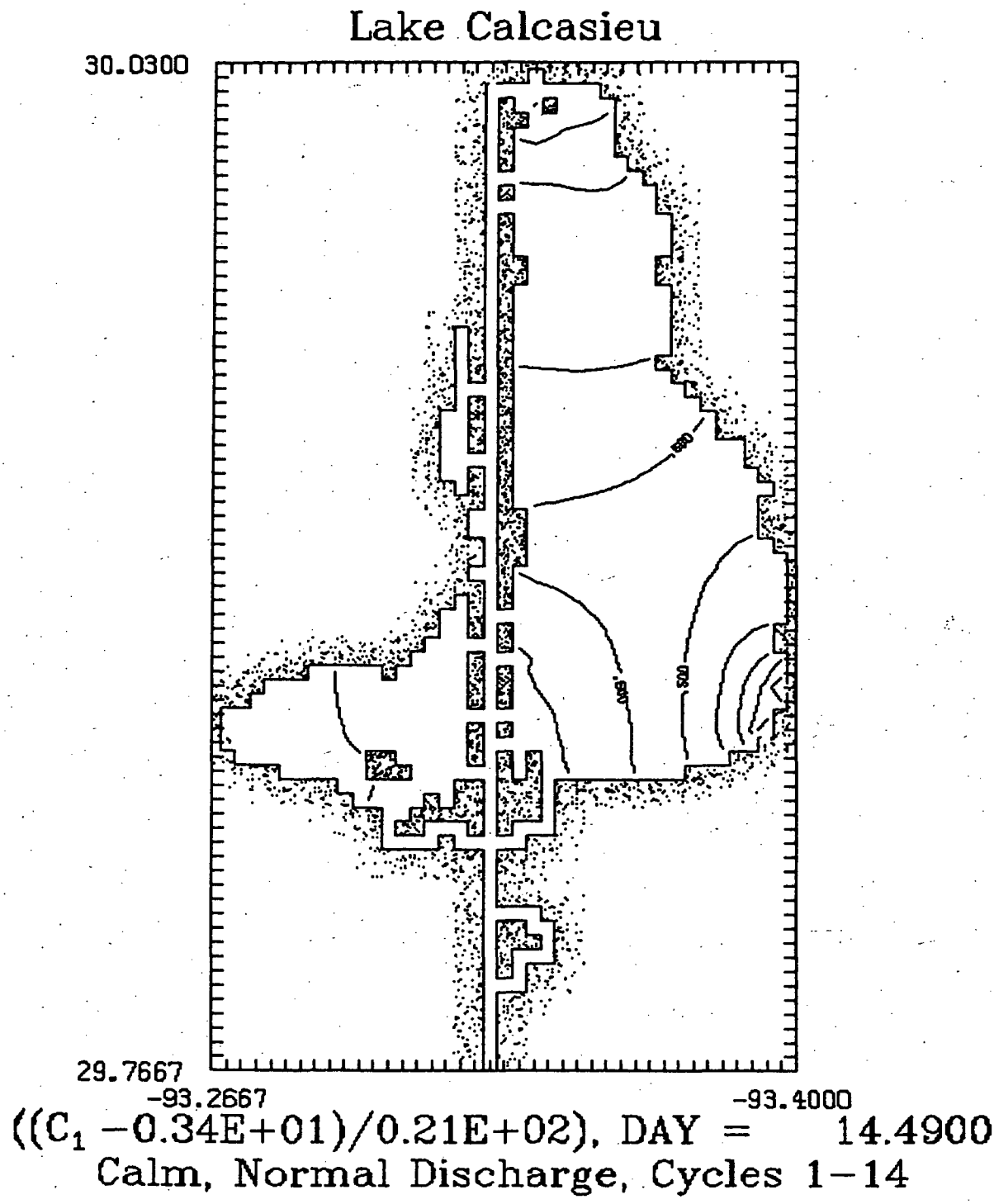

Fig. 1. Case 1 (no winds; mean river discharge; diurnal tides): Tidally-averaged salinity concentrations, averaged over the 14th tidal cycle. Normalized contours (0.1 - 0.9) indicate salinity concentrations ranging from 5.5 - 22.3 ppt.

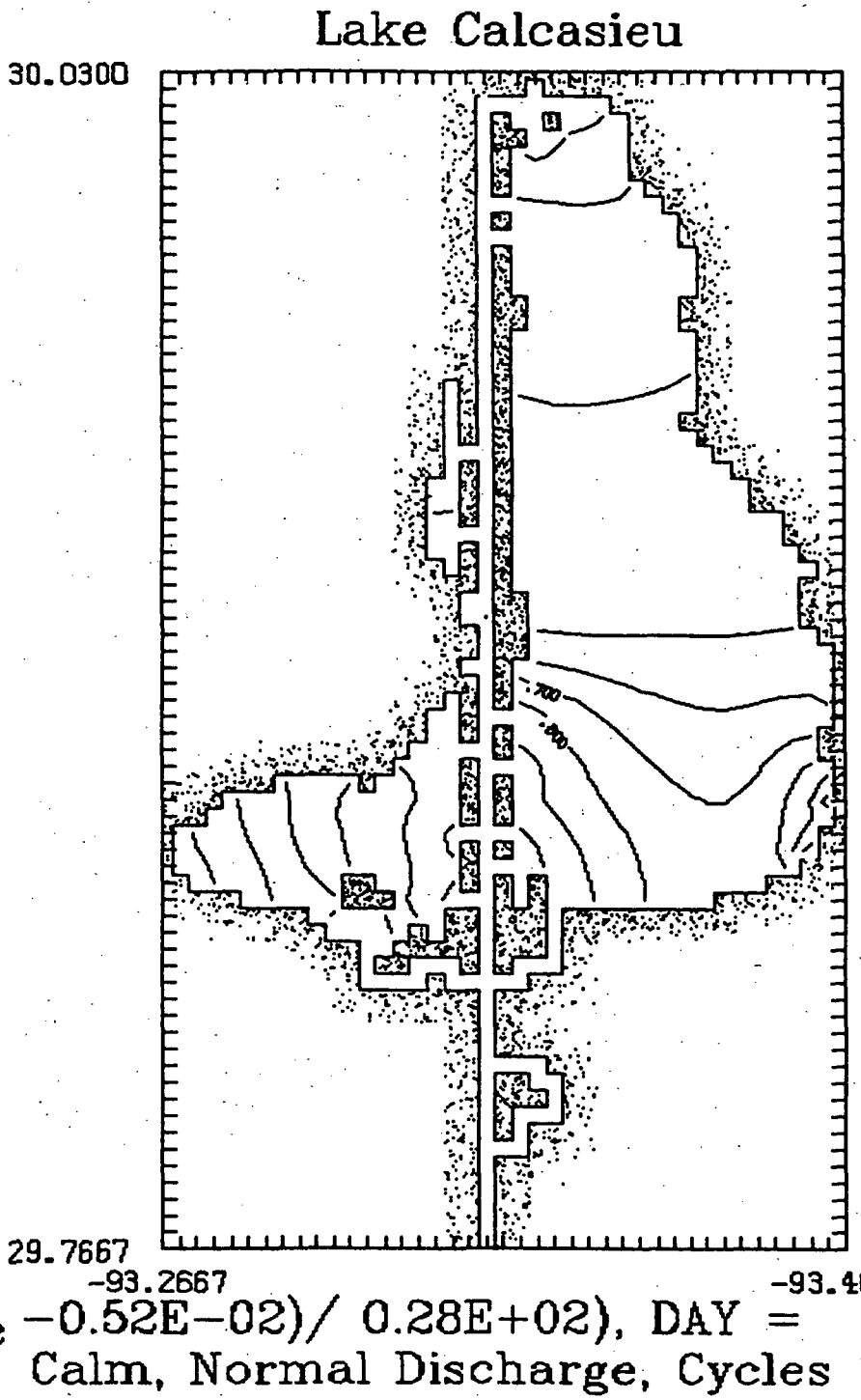

Fig. 2. Case 1 (no winds; mean river discharge; diurnal tides): Instantaneous suspended sediment concentrations. Normalized contours (0.1 - 0.9) indicate sediment concentrations ranging from 54.8 - 77.2 ppm.

ORIGINAL PAGE IS
OF POOR QUALITY

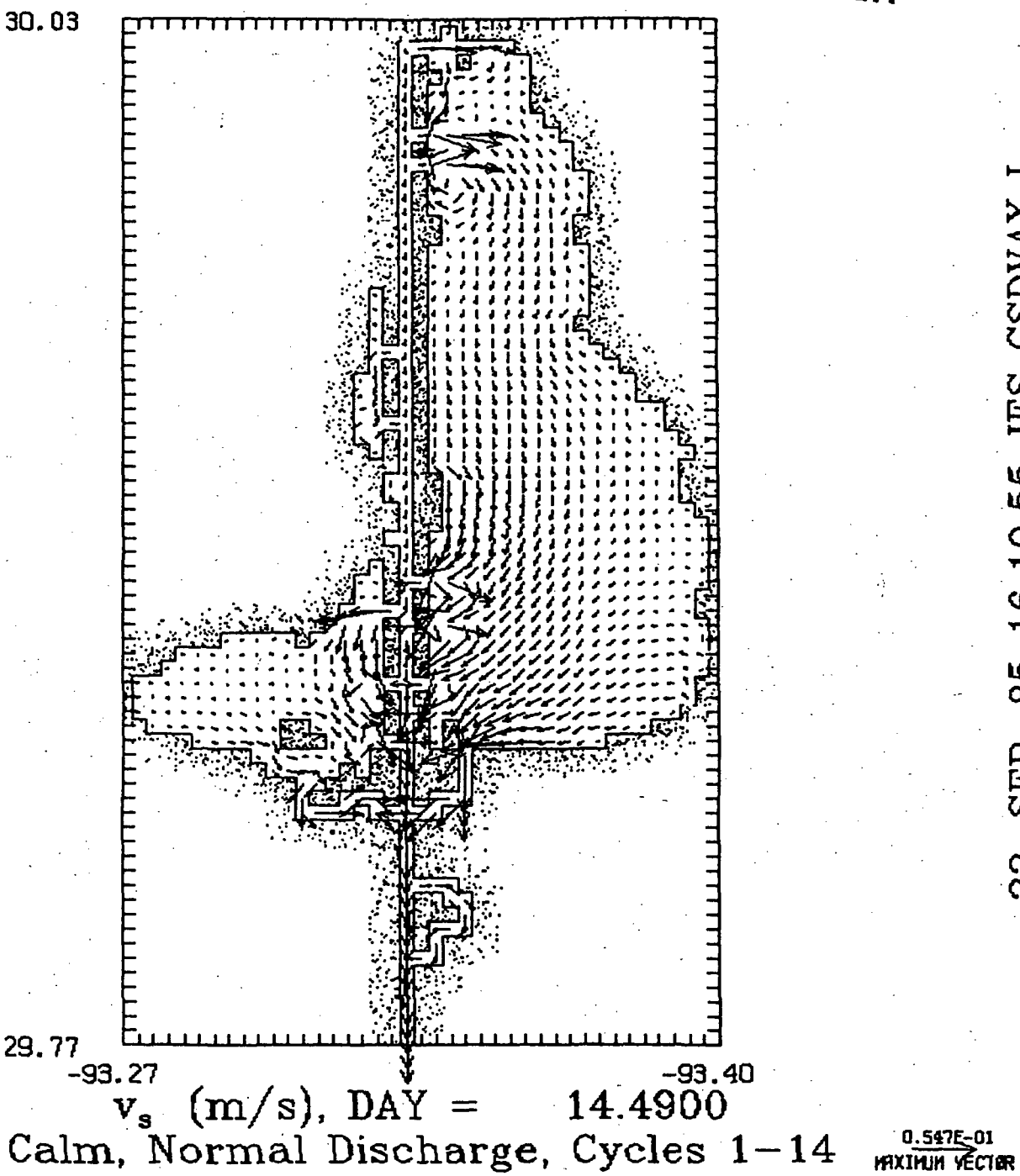

Fig. 3. Case 1 (no winds; mean river discharge; diurnal tides): Tidally-averaged vectoral representation of the depth-averaged (Stoke's) residual circulation averaged over the 14th tidal cycle.

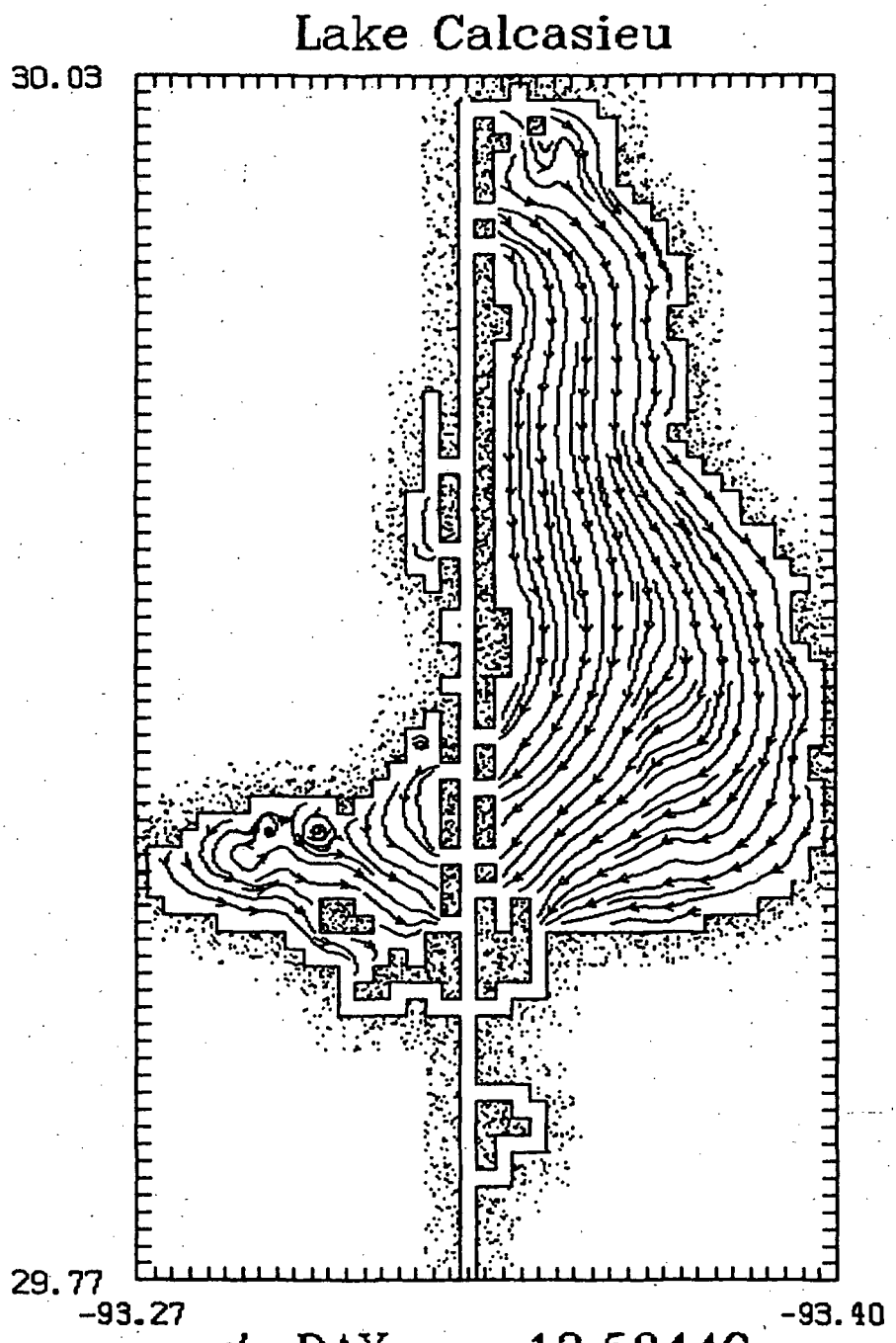

Fig. 4. Case 2 (10 m/s north winds; mean river discharge; diurnal tides): Instantaneous streamline representation of the circulation.

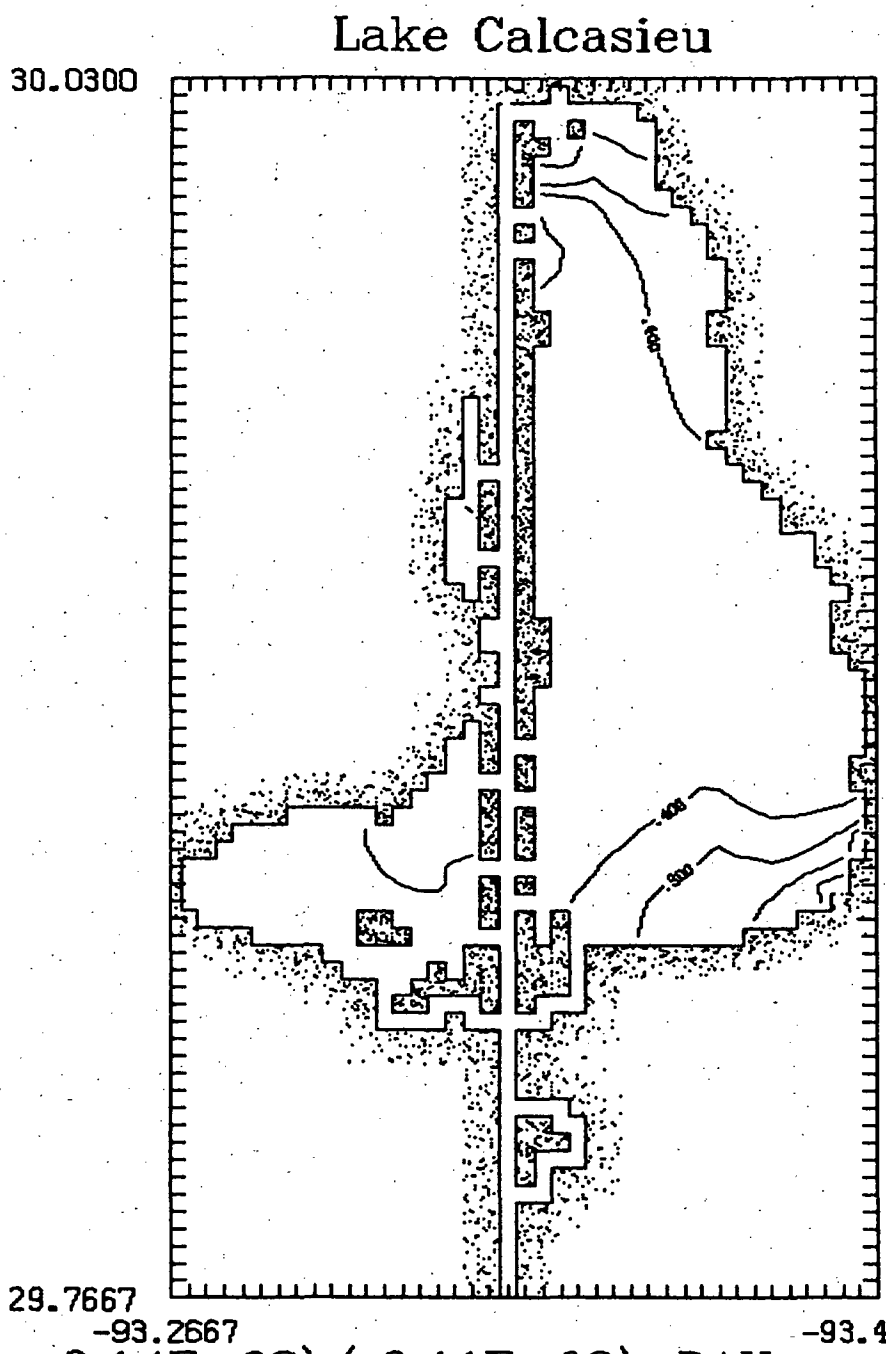

Fig. 5. Case 2 (10 m/s north winds; mean river discharge; diurnal tides): Tidally-averaged salinity concentrations, averaged over the 14th tidal cycle. Normalized contours indicate salinity concentrations ranging from 15.1 - 23.9 ppt (0.1 - 0.9)

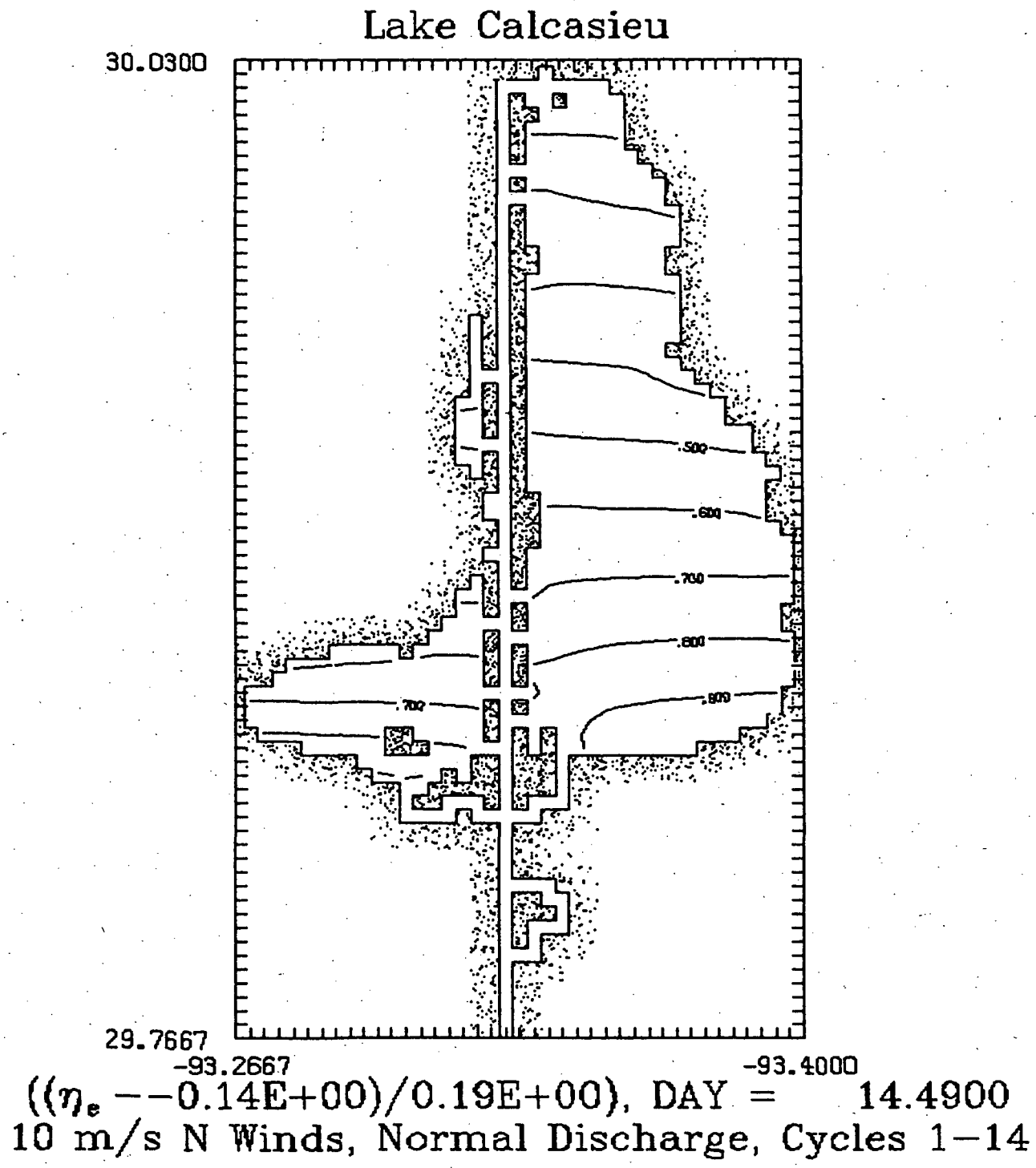

Fig. 6. Case 2 (10 m/s north winds; mean river discharge; diurnal tides): Tidally-averaged water elevations averaged over the 14th tidal cycle. Normalized contours (0.1 - 0.9) indicate elevations ranging from 0.2 - 0.3 m.